IMPROVEMENT OF SIGNAL-TO-NOISE RATIO

IN UTERINE EMG RECORDINGS

A Thesis

by

LUI CHENG

Submitted to the Office of Graduate Studies of
Texas A&M University
in partial fulfillment of the requirements for the degree of

MASTER OF SCIENCE

December 2003

Major Subject: Biomedical Engineering

IMPROVEMENT OF SIGNAL-TO-NOISE RATIO

IN UTERINE EMG RECORDINGS

A Thesis

by

LUI CHENG

Submitted to Texas A&M University
in partial fulfillment of the requirements
for the degree of

MASTER OF SCIENCE

Approved as to style and content by:

Charles Lessard (Chair of Committee)	Hsin-I Wu (Member)
Stephen Crouse (Member)	William Hyman (Head of Department)

December 2003

Major Subject: Biomedical Engineering

ABSTRACT

Improvement of Signal-to-Noise Ratio in Uterine EMG Recordings.

(December 2003)

Lui Cheng, B.S., Texas A&M University

Chair of Advisory Committee: Dr. Charles Lessard

The objective of this study is to remove or, at least, reduce the noise in uterine EMG recordings, which at their present noise level render the data unusable. Predicting when true labor will start and recognizing when labor actually starts are important for both normal and complex pregnancies. For normal pregnancy, the prognosis of labor is important for reducing unnecessary hospital costs. About 10% of the four million babies born each year in the United States are born prematurely. At $1,500 a day for neonatal intensive care, this comprises national health care expenses of well over $5 billion. Spectral analysis, filter design, and 1/3 octave analysis were applied to analyze the uterine EMG recordings. Signal-to-noise ratio was increased with IIR Butterworth bandstop filter. The spectral band between 0.25 and 0.4 Hz shows matching of the Toco belt via spectral analysis. Nevertheless, 1/3 octave analysis gives the highest correct detection percentage compare with frequency analysis and filter design.

To my parents and sisters.

ACKNOWLEDGEMENTS

This study would not have been completed without the help, support and encouragement of many individuals. I would like to take this opportunity to express my thanks and sincere appreciation of their efforts.

I am indebted to Dr. Charles Lessard for his guidance throughout the course of my master's degree program. This thesis could not have been completed in a timely manner without his encouragement, advice and assistance. His broad knowledge has been an important resource to me over these past years.

I wish to extend a special thanks to my graduate committee: Dr. Hsin-i Wu and Dr. Steve Crouse. I am grateful for their interest in my research efforts and insights they provided.

This study is in collaboration with the University of Texas Medical Branch at Galveston, Texas and Fairway Medical Technology, Inc. in Houston, Texas. Special thanks go to John Fuqua, Clinical Research Coordinator at Fairway Medical Technologies, for giving me permission to have access to data obtained as part of electromyographic (EMG) studies being conducted by Fairway at the University of Texas Medical Branch at Galveston.

Finally, I would like to express my deepest gratitude to my sisters, Kam Cheng and Man Cheng, and my American parents, Jim and Marilyn Caton for their tremendous care and spiritual support. Without their understanding and encouragement, I would not have had a momentum to complete my degree.

TABLE OF CONTENTS

Page

LIST OF TABLES

LIST OF FIGURES

Figure Page

INTRODUCTION

This study is in collaboration with the University of Texas Medical Branch at Galveston, Texas (UTMB) and Fairway Medical Technology, Inc. Houston, Texas (Fairway). The overall goal of the study is the development of a medical device that can accurately identify, detect and analyze uterine smooth muscle contraction from pregnant women in labor. Preliminary recordings from a crude prototype system produced uterine EMG signals that were very contaminated with noise. The uterine EMG signals were collected at the UTMB OB-GYN department, using a prototype Uterine EMG recorder and a personal computer. The sanitized (removal of patient personal identification, e.g., name, SSN, etc.) data files (N=38) were sent to Dr. Lessard, Biomedical Engineering Department at TAMU for analysis.

Preliminary evaluation of the signals at UTMB showed that changes in uterine myoelectric activity, which correspond to the signals of a tocodynamometer (Toco belt), follow the progression of the pregnancy and the onset of labor [unpublished paper by Dr. Garfield]. The specific goals of the UTMB research are:

1. to determine measurable increases in the following parameters which occur during the pregnancy leading to labor: amplitude and power of bursts, high frequency content of action potential waveforms, rate of burst production, and duration of bursts,

---

This thesis follows the style and format of *IEEE Transactions on Biomedical Engineering.*

2. to determine if observable increases in energy of the electrical activity and the increased high-frequency content of the action potentials are favored by the changes occur in the electrical properties of the myometrium (the muscular outer layer of the uterus) during labor to increase current flow in the myometrial smooth muscle, and
3. to replace the Tocodynamometer system with the less painful, noninvasive Uterine EMG Contractility Monitor.

The primary objective of this study is to remove or, at least, reduce the noise in the uterine EMG recordings, which at their present noise level render the data unusable. A secondary goal is to evaluate and develop a very narrow band digital filter in order to increase the signal-to-noise ratio.

BACKGROUND

Identification of the onset of true labor has been one of the most difficult and critical challenges facing obstetric practitioners in maternity care. Predicting when true labor will start and recognizing when labor actually starts are important for both normal and complex pregnancies. For normal pregnancy, prognosis of labor is important for reducing unnecessary hospital costs. These costs are due to risky childbirth happened before the mother arrives at the hospital, or are the outcome of false labor. Preterm birth is the most common pregnancy complication for complex pregnancies, with 20% of all pregnant women at high risk. About 10% of the four million babies born each year in the United States are born prematurely [1], [2]. At $1,500 a day for neonatal intensive care, this comprises national health care expenses of well over $5 billion [3]. Also, preterm birth is the single most significant contributor to infant mortality and morbidity. Early detection is one of the most feasible means to treating preterm birth. Medical specialists can try to inhibit the labor process if preterm labor is detected early; if unsuccessful, they are better prepared to handle the premature newborn.

Diagnosis of Labor

Today, labor remains a clinical diagnosis. Even though several methods have been used to monitor labor, they are subjective and do not provide accurate differentiation between true and false labor or predict when labor will occur. Currently, the most important key to preventing preterm labor has been constant contact and care

from health care practitioners [4]. Although several methods can identify signs of ongoing labor, none of the methods offer objective data that can accurately predict labor over a broad range of patients. The methods range in complexity from simple patient self-awareness to complex electronic pressure sensors. Table 1 lists the current methods with relative degree of accuracy and if the method is invasive or not [5]. The current state of labor monitoring can be summarized as follows:

(a) current methods are subjective;

(b) intrauterine pressure catheters provide the best information but their use is limited by invasiveness and need for ruptured membranes;

(c) present uterine monitors are uncomfortable and inaccurate;

(d) no method has been successful at predicting preterm labor;

(e) no method has led to effective prevention of preterm labor.

Table 1

Current methods used in uterine monitoring or screening of labor

Method	Accuracy	Invasive
1. Monitoring of contractions in combination with pelvic examination	Moderate	No
2 .Monitoring the state of the cervix	Moderate	No
3. Symptomatic self-monitoring	Low	No
4. Intrauterine pressure monitor	High	Yes
5. External uterine monitor (tocodynamometer)	Erratic	No
6. Ultrasound monitor	Mixed	No
7. Endovaginal ultrasonography	High negaive predictive values	No
8. Fetal fibronectin screening test	High negaive predictive values	No
9. Salivatory estriol test	High negaive predictive values	No

Intrauterine Pressure Catheters

Early detection of preterm labor is difficult because initial symptoms and signs are often mild and may occur in normal pregnancies. Thus, many healthy women will report symptoms during routine prenatal visits, whereas others predetermined for preterm birth may dismiss the early warning signs as normal in pregnancy. Among the current methods, intrauterine pressure catheters provide the best information concerning uterine contractions, but the invasive instrument can increase the risk of infection since it requires rupture of membranes. Intrauterine pressure catheters also do not provide information about cervical function.

External Uterine Monitor

Tocodynamometers (Tocos) are external pressure measurement devices that are used to detect changes in abdominal contour as an indirect indication of uterine contraction. The primary advantage of a tocodynamometer is that it does not require an invasive probe, which allows the device to be used for most pregnancies without risk to the fetus or the mother. External tocodynamic monitoring devices are used in over 90% of all hospital births. Physicians have been quick to adopt Tocos with little risk. However, these instruments have not changed treatments for preterm labor. Tocodynamic devices have one major drawback, “accuracy”. Several variables affect the measurement of uterine contractions, such as instrument placement, amount of subcutaneous fat, and uterine wall pressure. Also, the use of external tocodynamometry is limited to obtaining the frequency of contractions and does not include any direct or

indirect measure of functional interest, such as, force or efficiency of the contraction. Nevertheless, the advantage of a noninvasive method for providing uterine contraction data has led to its widespread adoption despite known limitations.

Home Uterine Activity Monitoring

Home uterine activity monitoring (HUAM) has been advocated as an ambulatory screening test for labor in high-risk women [6], [7]. The home tocodynamometer consists of a pressure sensor that is held against the abdomen by a belt and a recording/storage device that is carried by a belt or hung from the shoulder. The patient typically records uterine activity for 1 hour, twice a day, while performing routine activities. The stored data are transmitted via telephone to a practitioner, where a receiving device prints out the data. Patients are often contacted by, or have access to, personnel who can address monitoring problems. The sensitivity and specificity of HUAM are uncertain, due to lack of data and the absence of a reference standard. Also, HUAM was no better at lowering the frequency of preterm birth than weekly contact with a nurse.

Monitoring the State of Cervix

The state of cervix as determined by digital examination is used clinically as a predictor of labor. Yet, the relationship between softening, effacement, dilation of the cervix and changes in uterine contractility varies. In fact, uterine activity and changes in the cervix occur separately. Measurement of the length of the cervix by endovaginal

ultrasonography has been used to predict premature labor [8]-[13]. However, the positive predictive value is only around 25% (based on ultrasound, 75% of patients with a shortened cervix will deliver at term).

Other Monitoring Methods

Assessment of cervical or vaginal fetal fibronectin has been suggested as a screening method for patients at risk of premature labor. Results from several studies [14]-[18] have shown that fetal fibronectin might be useful in predicting actual premature labor. Other studies [17] found that fetal fibronectin had limited predictive value. The value of the fetal fibronectin assay lies in its high negative predictive value; it has the ability to identify patients who will not deliver prematurely. Similarly, salivary estriol has been shown to be useful because of its high negative predictive value [19], [20].

Of the methods discussed above, the intrauterine pressure method provides the best information, but not without increased risk after rupture or puncture of the membranes, thus increasing the chances of infection and other more severe complications. Thus, it would be useful if the progress or evolution of labor could be measured directly and noninvasively.

The Myometrium

Currently, in both non-pregnant patients where hyper-contractility is associated with dysmenorrhea (painful menstruation) and in pregnant women where the uterus is

sometimes active before term, there is no objective and noninvasive method in which to evaluate the contractility of the uterus. Normally the uterus is quiescent in non-pregnant women and during most of pregnancy. Yet, at the end of pregnancy the myometrium experiences a series of changes that lead to increased reactivity and synchronous, rhythmic uterine contractions (labor) [21]. Since there are some minor spontaneous uterine contractions at all times throughout pregnancy, it is often not possible to distinguish between physiologic activity and term or preterm labor.

Uterine contractions are a necessity, but not a sufficient condition to determine the onset of labor [22]. Therefore, monitoring of uterine contractions does not help to identify patients who are likely to deliver prematurely. Over the last decade, uterine and cervical electrical activities have become the object of many research studies [23]-[25], which offer a better intuition into the pregnant uterus and the process of labor. Many studies have recorded uterine myometrial electrical activity by use of electromyography, where electrodes were placed directly on the uterus [23], [26]-[31]. These studies show that there was minimal uterine electrical activity, consisting of infrequent and low-amplitude EMG bursts, throughout most of pregnancy. When bursts occurred before onset of labor, they often corresponded to the perception of contraction by the woman. During term and preterm labor, bursts of EMG activity were frequent, of large amplitude, and correlated with the large changes in the intrauterine pressure and pain sensation.

Electrical Properties of the Myometrium

Contractions of the uterus are dependent on the generation and propagation of action potentials of the muscles in the myometrium [26], [32], [33]. Unlike single action potentials that initiate contractions of striated muscle, action potentials in the myometrium occur in groups, known as “bursts”. The frequency and duration of the bursts prescribe and are directly proportional to the frequency and duration of the contractions, respectively, whereas the propagation of action potentials and the recruitment of additional muscle cells are related to the amplitude of the contraction [33].

The sequence of contraction and relaxation of the myometrium results from the cyclic depolarization and repolarization of the membranes of the muscle cells. The spontaneous electrical discharges in the muscle from the uterus consist of intermittent bursts of spikelike action potentials [33]-[39]. Uterine volume (chronic stretch) and ovarian hormones (principally estrogen) contribute to the change in action potential shape through their effect on the resting membrane potential [40]-[42]. A single spike can initiate a contraction, but multiple, coordinated spikes are needed for forceful and maintained contractions [34]. As in other excitable tissues, the action potential in uterine smooth muscle results from voltage – and time – dependent changes in membrane ionic permeability [43].

Studies of isolated myometrial tissues using microelectrodes or extracellular electrodes showed that the temporal association between electrical events and

contractions [27], [29], [44]-[55]. In all species, each contraction was accompanied by a burst of action potentials (Figure 1) that started slightly earlier than the contraction.

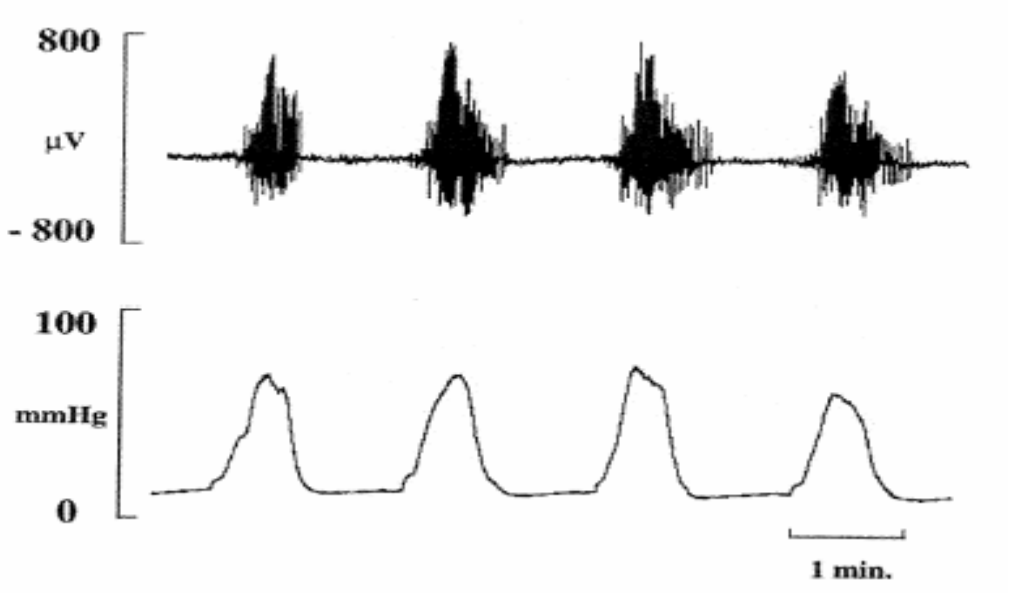

Figure 1. Electromyographic activity recorded directly from the uterus (top), and intrauterine pressure (bottom) obtained from a pregnant rat during labor [5].

The frequency, amplitude, and duration of contractions are determined, respectively, by the frequency of action potentials within a burst, the duration of a burst, and the total number of cells that are active simultaneously [34]. The frequency of the action potentials within a burst first increases and then decreases. The burst stops before the uterus has relaxed [34]. The electrical and mechanical activities of the myometrium have been recorded in animals of various species by many investigators [26], [29], [45]-[52], including humans [29], [40]-[52], [56]. Many studies [21], [57]-[60] provide convincing data that uterine EMG activity can be assessed from abdominal surface measurements.

Uterine Electromyography: EMG Recordings and Uterine Contractile Activity

A recent study by Garfield R. E. *et al.* [5] showed that abdominal surface recording of uterine electrical activities corresponds to the electrical activity of the uterus. The conclusion made by the author is based on the following subjective observations:

a) action potential bursts obtained from the abdominal surface almost perfectly matched burst occurring in the uterus;
b) increases and decreases in electrical bursts at both sites were accompanied by similar changes in intrauterine pressure;
c) changes in activity during term and preterm labor were detected simultaneously from the uterus and abdominal surface;
d) pharmacologic stimulation or inhibition resulted in similar changes in recordings from both sites [58];
e) cardiac action potentials did not interfere with uterine or abdominal recording.

Researchers of this study concluded that recording of uterine EMG from the abdominal surface is a reliable method to follow the evolution of uterine contractility during pregnancy. Analysis of EMG activity can be used to characterize and evaluate uterine contractions during term and preterm labor. This noninvasive technology could be useful in the treatment of labor and its complications.

METHODS

The aim of this study is primarily to analyze digitized uterine contractions from electromyogram (EMG) data collected from patients in labor at the University of Texas Medical Branch at Galveston, TX. The original task is directed at removing or at least reducing the noise level from the EMG data files. The noise may come from peristaltic movement, fetus movement, and leg movement of the mother and etc. The uterine EMG signals were sampled at a rate of 100 samples-per-second (sps) and stored as ASCII formatted data files. The digitized data are imported to the "DADiSP" digital signal processing software (DSP Development Corporation, Cambridge, MA). Several DADiSP programs were developed to evaluate removal of extraneous noise through the following methods:

1. Regression Approach
2. Spectral Analysis
3. Digital Filtering Approach
4. Running Calculation of the Signal-to-Noise Ratio
5. 1/3 Octal Analysis

A brief description of each approach will be presented. Figure 2 shows the general approach using the DADiSP programming.

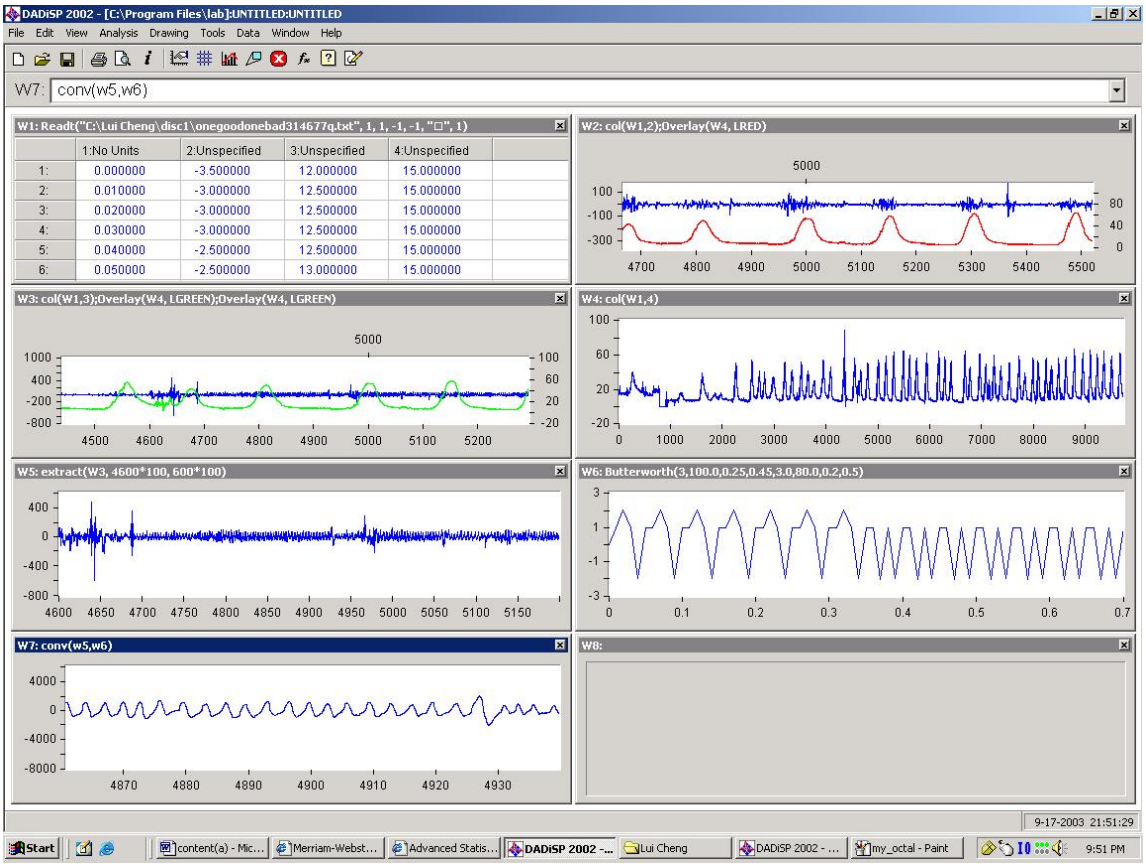

Figure 2. The general worksheet from the DADiSP digital signal processing software. The program is for processing the surface EMG data from a patient in labor.

The multi-channel data is loaded into Window 1, and then the channels are separated in Windows 2 (Good EMG Channel), Windows 3 (Bad EMG Channel), and Windows 4 (Toco Belt Channel), respectively (Fig. 2).

Regression Approach

Since the uterine EMG records are very much like sinusoidal signals, the first method attempted was regression model, trying to find a parametric equation to fit the data. Noisy portions of record containing no visible EMG signals during contraction

were fitted with a sinusoidal (sum of sines) model. Figure 3 shows a noise segment of the data in blue with the corresponding regression model of the noise (red trace) [61].

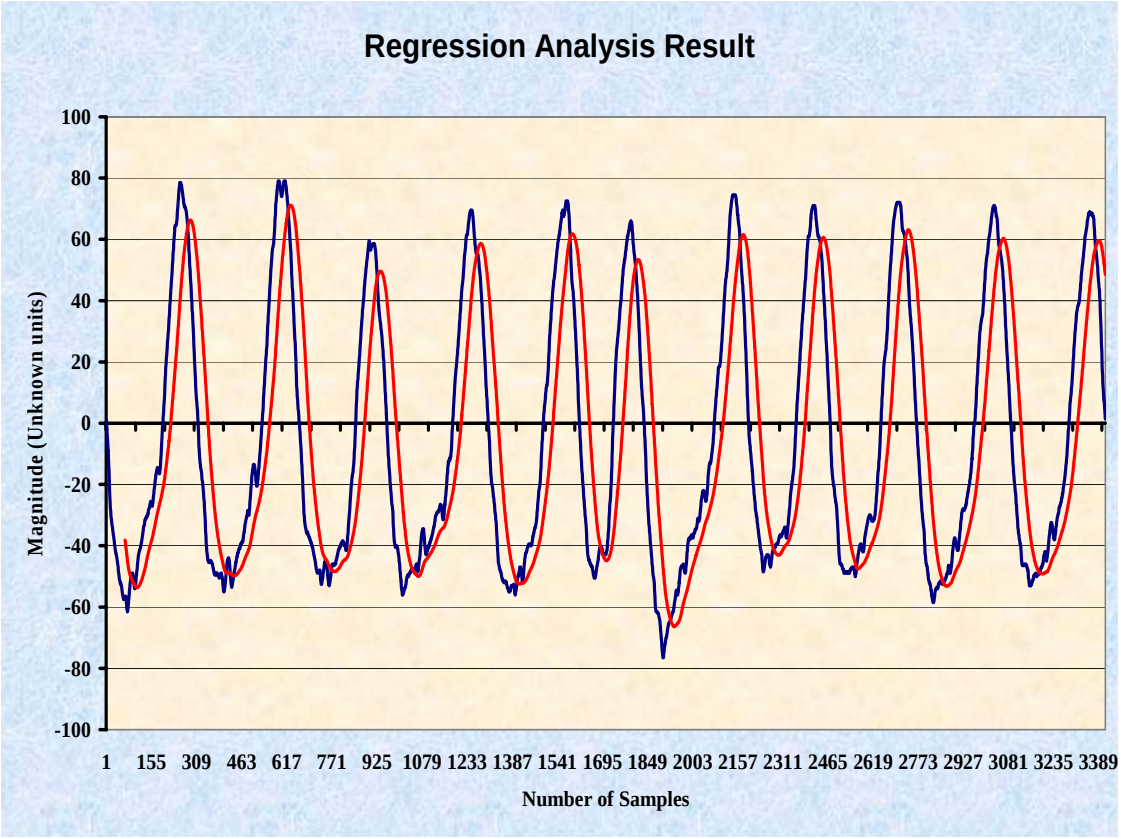

Figure 3. Regression model. The noise segment of the data is the blue trace and the corresponding regression model of the noise is the red trace [61].

Then, the model was consecutively subtracted from the original recording to reduce the extraneous noise, which acts as a filter.

Digital Filtering Approach

Digital filtering approach used various digital filters to remove the noise components and accentuate the true EMG components. Several types of filters were used

on bad channel of EMG data and compared with good channel EMG data. Types of filter included:

1. Finite Impulse Response (FIR) Filters
    a. Bandpass
    b. Bandstop
2. Infinite Impulse Response (IIR) Filters
    a. Butterworth
        i. Bandpass
        ii. Bandstop
    b. Chebychev
        i. Bandpass
        ii. Bandstop

Spectral Analysis

The spectral analysis takes advantage of DADiSP's "Ravel" command which segments the data. The "frequency" program (Fig. 4) was developed to segment the data into 20-second segment (2000 samples per segment), which are overlapped by 75% (meaning the 20-second window is moved forward by 5-second – 500 samples). The samples are modulated with a Kaiser window function in order to reduce the side-lobe spectral leakage, and the Power Spectral density is calculated.

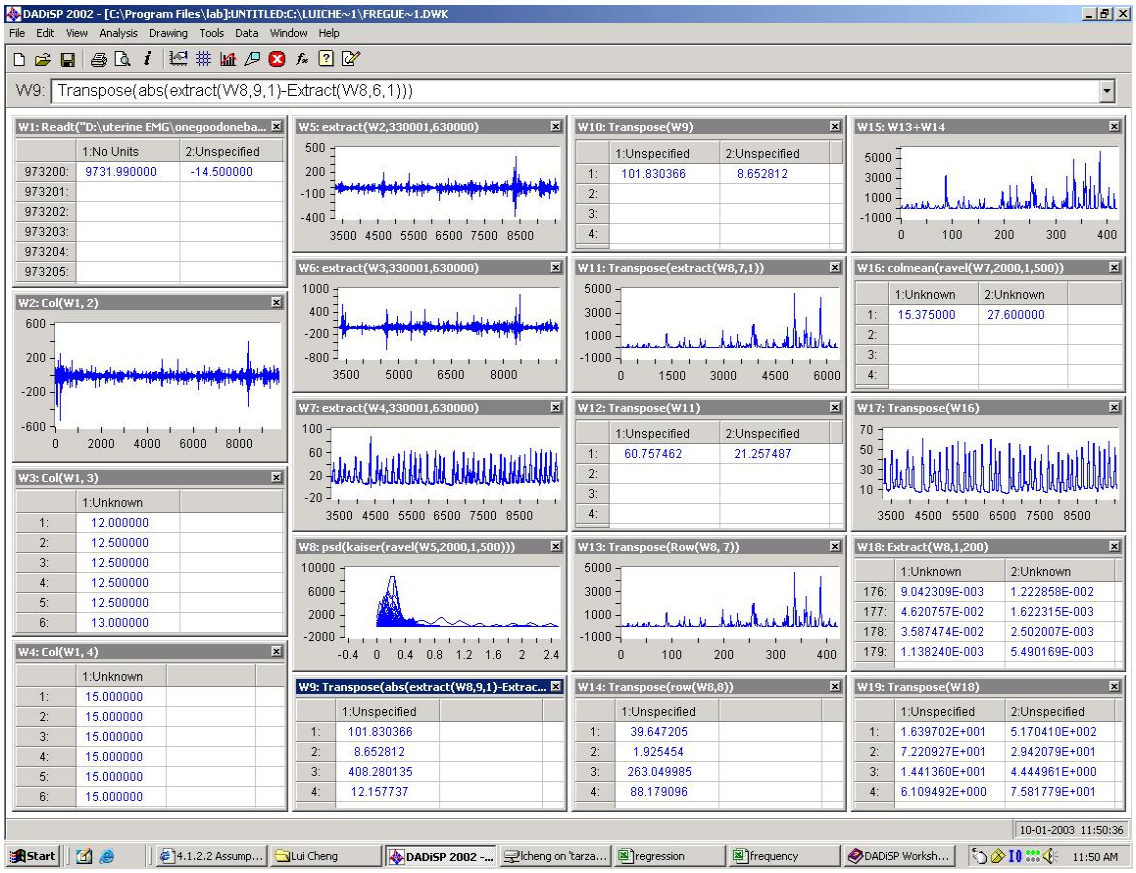

Figure 4. DADiSP "frequency" program. The frequency program was developed to calculate the power spectral density function for 20-second segments of the raw EMG. Segments were overlapped by 25%.

Introduction to Octave Analysis

Octave analysis displays a signal's frequency characteristics in frequency bands where each frequency band covers an octave -- a band from frequency *f* to frequency 2*f* [62], for instance, 250 Hz to 500 Hz. Each band, therefore, occupies a bandwidth that's twice as wide as the previous band and half as wide as the next band. Octave analysis could be thought as passing a signal through a series of band-pass filters, each covering one octave. Figure 5 shows how octave analysis divides the audio-frequency band into octaves.

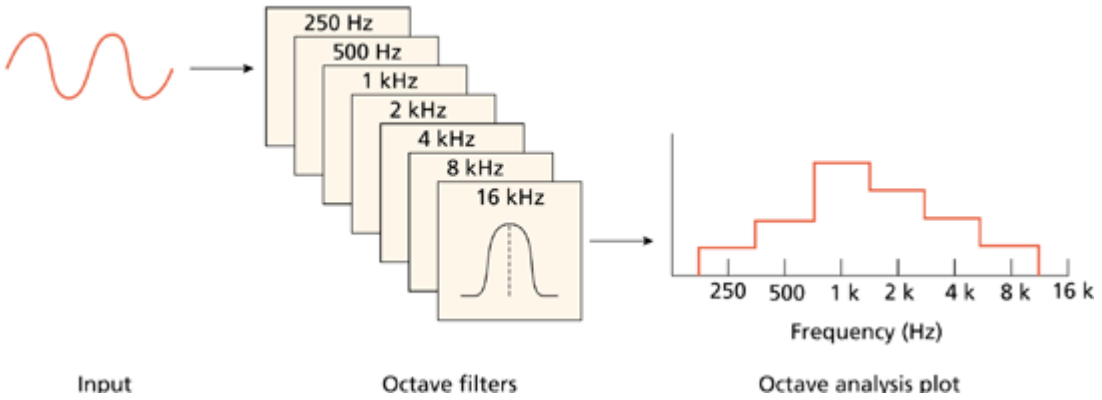

Figure 5. Octave analysis passes a time-domain signal through a series of octave (or a fraction of an octave) band-pass filters, producing an octave plot [62].

Octave analysis shares some similarities with power-spectral analysis, but in spectral analysis all frequency bands (bins) occupy equal bandwidth. For example, in a 1000-point FFT that covers DC to 10 kHz, each bin occupies 10 Hz. The frequency resolution is linear over the entire range. Because of its log scale, octave analysis can show results over multiple octaves, allowing ones to see and compare signal levels over a nonlinear frequency range.

Each octave band's frequency range falls between f_l and f_h, where $f_h=2f_l$. The octave's 2:1 ratio sets a geometric spacing between octave bands, meaning that the bandwidth of each octave maintains a constant ratio with its geometric mean. The following equation could be used to calculate the geometric mean of the octave's end frequencies:

$$Meanfrequency = \sqrt{f_h x f_l}$$

1/3 Octave Analysis

The spectrum could be divided into geometrically equal subdivisions of each band for greater resolution. Hence, the 1/3 octave analysis, modified octave analysis used, divides each octave band into 3 equal subdivisions. For instance, an octave band of 0.1-0.2 Hz, the first 1/3 octave band is 0.1-0.1333 Hz, the second 1/3 octave band is 0.1333-0.1667 Hz, and the third one is 0.1667-0.2 Hz.

Based on the frequency analysis, the significant part of the power spectrum density of human uterine electromyographic activity has a very low range of frequency of 0.2 Hz - 0.5Hz. So, for 30 seconds resolution of 1/3 octave analysis, we set the first octave band from 0.1 Hz to 0.2 Hz, the second from 0.2 Hz to 0.4 Hz, and the third from 0.4 to 0.8 Hz and up to 1 Hz. (Notice that it does not have a complete octave band starting from 0.8 Hz). Each octave band was divided it into 3 equal sub-bands, namely 1/3 octave in this case. For the first octave band, each 1/3 octave contains 1 subdivision. However, each 1/3 octave of second octave band contains 2 subdivisions. The detail calculation of the distribution of octave band is done in Excel sheet as shown in Table 2. The DADiSP program of 1/3 octave analysis is shown in Figure 6.

Table 2

Excel sheet of 1/3 octave band calculation

Octave Band	Frequency Range (Hz)	Equally divided subdivisions		1/3 Octave 1st	1/3 Octave 2nd	1/3 Octave 3rd	Number of subdivisions in each 1/3 octave band
1	0.1	0.100	0.133	I			
	↓	0.133	0.167		I		1
	0.2	0.167	0.200			I	
2	0.2	0.200	0.233	I			
	↓	0.233	0.267	I			
		0.267	0.300		I		2
		0.300	0.333		I		
	↓	0.333	0.367			I	
	0.4	0.367	0.400			I	
3	0.4	0.400	0.433	I			
	↓	0.433	0.467	I			
		0.467	0.500	I			
		0.500	0.533	I			
		0.533	0.567		I		
		0.567	0.600		I		4
		0.600	0.633		I		
		0.633	0.667		I		
		0.667	0.700			I	
		0.700	0.733			I	
	↓	0.733	0.767			I	
	0.8	0.767	0.800			I	
4	0.8	0.800	0.833	I			
	↓	0.833	0.867	I			8
		0.867	0.900	I			(not enough
		0.900	0.934	I			In this case)
	↓	0.933	0.967	I			
	1	0.967	1.000	I			

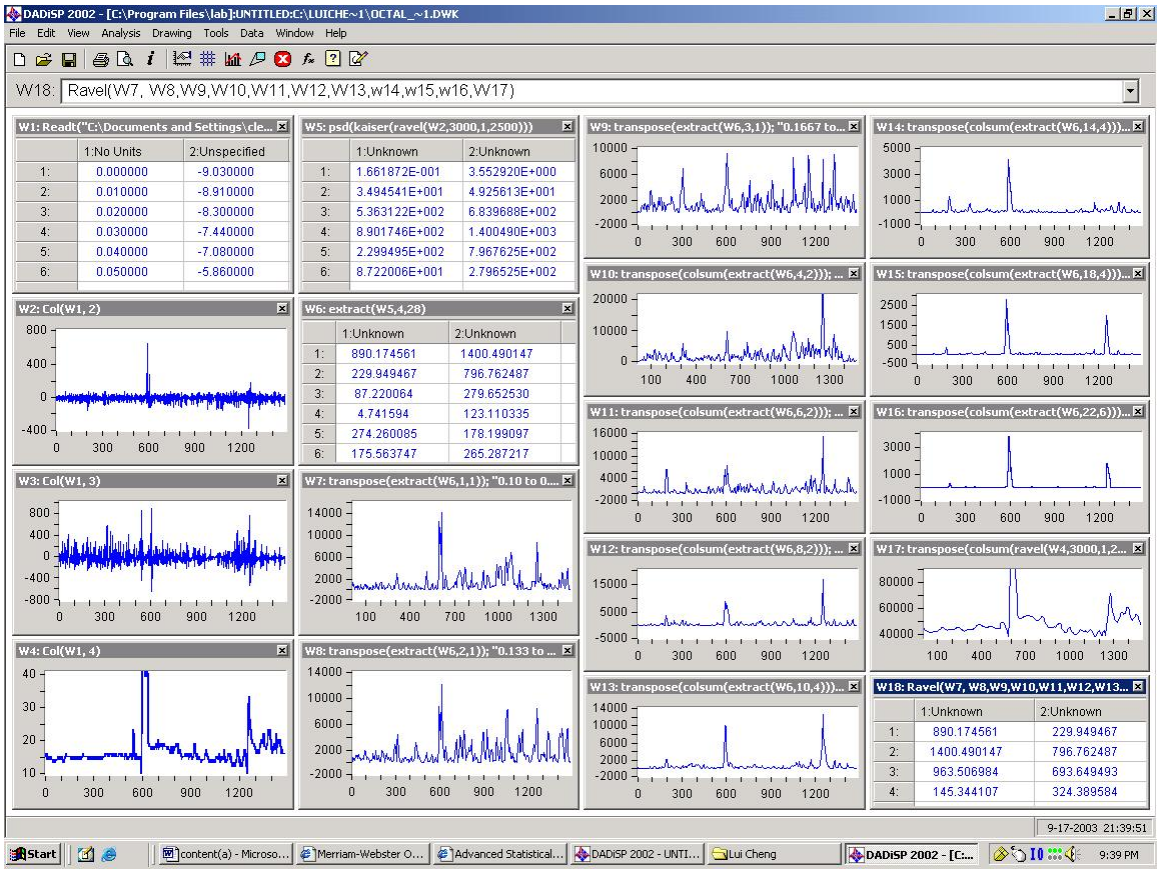

Figure 6. DASiSP program of 1/3 octave analysis.

In Window 5, the power spectral density function was performed on the good (or bad) EMG data for 30 seconds with 25 seconds overlapped (to better smooth the signal). Signals of frequency between 0.1 and 1 Hz were extracted out and put into Window 6. From Window 7 to Window 9, we performed the 1/3 octave analysis for the first octave band, 0.1 Hz – 0.2 Hz. The 1/3-octave analyses of the following octave bands were done in Window 10 through Window 16. The same power spectral density analysis was performed to channel 4 in Window 17, the Toco belt signal, for later comparison. In

Window 18, all the data was gathered and put into different columns and exported to Excel for graphic plotting.

Calculating Signal-to-Noise Ratio

The Signal-to-Noise ratio(s) (SNR) could be calculated by dividing the root mean square (RMS) value of the region of the noise segment from the RMS value of true EMG contraction between EMG activities.

$$\text{SNR} = \frac{RMS\ of\ true\ EMG\ contraction}{RMS\ of\ noise\ segment}$$

These segments are verified with the activity of the Toco belt. Corresponding segments were extracted from both good and bad data channels (Fig. 7).

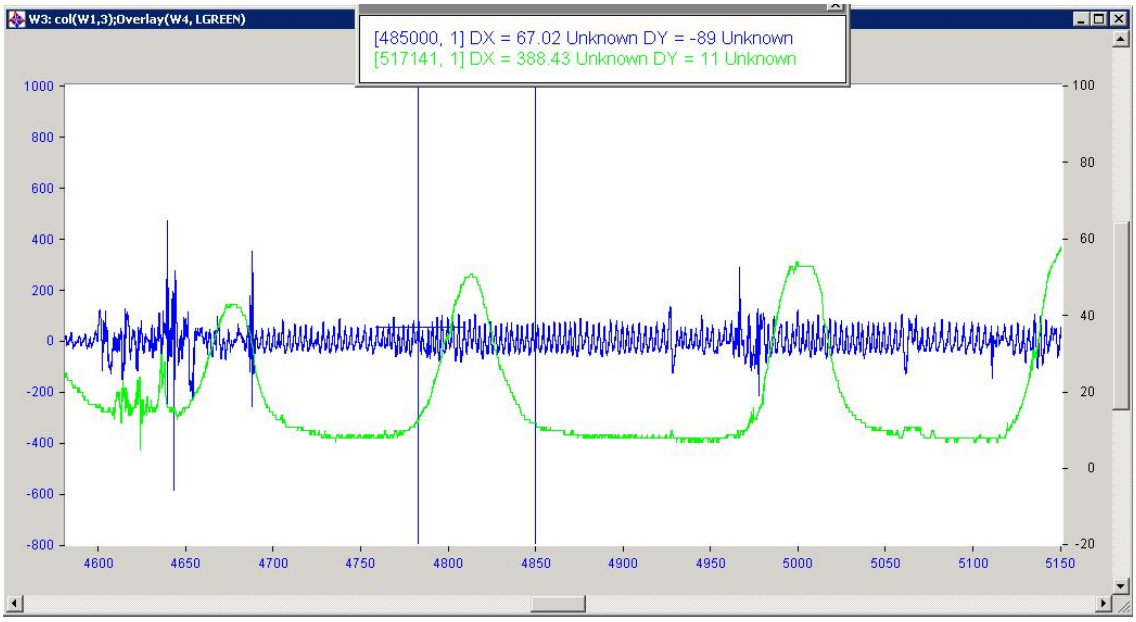

Figure 7. Raw EMG from channel 3. The trace is a segment of raw EMG contraction from channel 3 followed by the noise in the absence of any EMG signal between 4700 and 4950 seconds.

RESULTS AND DISCUSSION

Results

In this section, the results that we acquired via the various analytical approaches, i.e., regression analysis, power spectral analysis, digital filtering approach, the 1/3 octal analysis and calculating signal-to-noise ratio will be discussed. The results will be presented in chronological order and a comparison of uterine EMG detection to Tocodynamometer detection will be made in terms of Detection Accuracy

Regression Approach

The result of regression approach corresponds to what Lessard [64] found in his unpublished report. He found that regression model did not give any significant result since the noise does not seem to have been removed or reduced in the resulting EMG, the result is shown in Figure 8 [64]. Even if a perfect fit for this segment of noisy data was achieved, it would not fit the next one perfectly. So a regression model for each noisy data segment would have to be found and it would be very time consuming, and is not worth doing so.

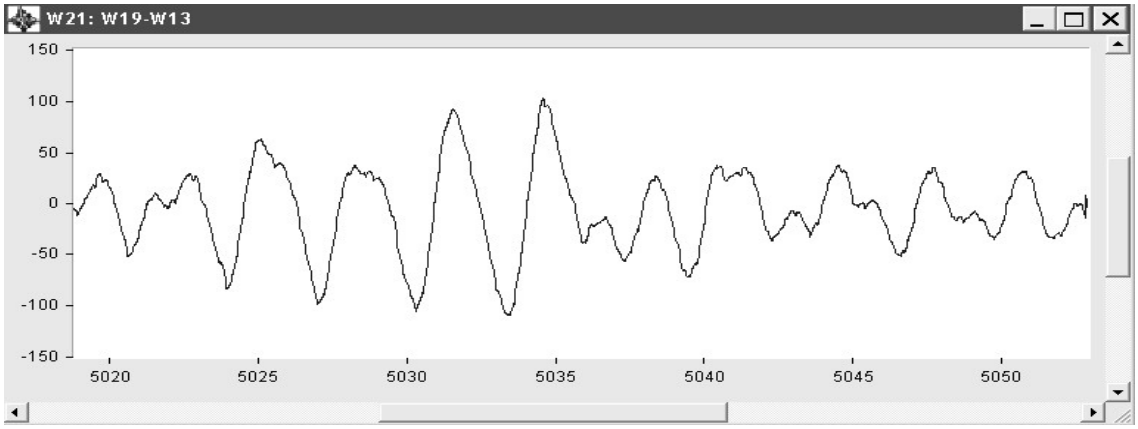

Figure 8. Result of the regression approach. The trace is the resulting EMG waveform after subtracting the regression model from the original EMG [64].

Digital Filtering Approach

Table 3 shows the comparison of average, standard deviation, and variance values of signal to noise ratio (SNR) of the bad signal after filtering with various filters. The “Channel 3 Original Data” column shows the SNR values of the raw data (before filtering), the next three columns are the values of the signal after filtering with “IIR Butterworth Bandstop Filter”, “IIR Butterworth Bandpass Filtershowed”, and “FIR Remex Exchange Bandpass Filter”, respectively. The results of visual comparison and SNR comparison shows that the IIR, Butterworth, Bandstop filter gives the best result, which improved the signal-to-noise ratio from 1.1613 to 1.5327.

Table 3

Comparison of signal-to-noise ratio of various filters applied to the bad data

	Channel 3 Original Data	IIR Butterworth Bandstop	IIR Butterworth Bandpass	FIR Remex Exchange Bandpass
Average SNR	1.1613	1.5327	1.1984	1.4667
Standard Dev.	0.4052	0.9575	0.4178	0.6441
Variance	0.1642	0.9167	0.1745	0.4148

Additionally, a second DADiSP "filter" program was developed accordingly using an 80-dB, IIR, butterworth, bandstop filter with center frequency at 0.325 Hz, low-frequency stop band at 0.2 Hz, and High-frequency stop band at 0.4 Hz. A running root mean square (RMS) of 1-second (100 samples) and 2-second (200 samples) were calculated for both good and bad channels (Figure 9).

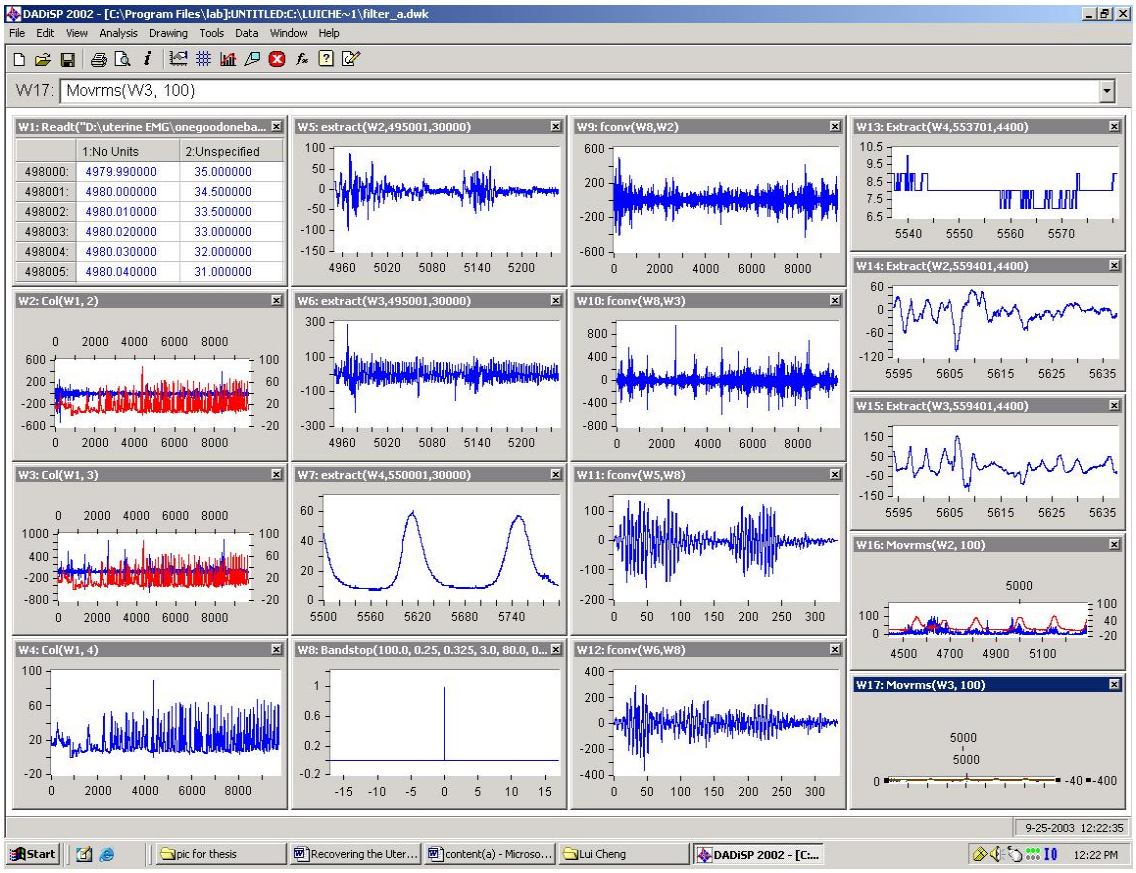

Figure 9. DADiSP "filter" program. Window 8 is the best IIR filter, which gave the best comparative result. The moving RMS value for every second and 2 seconds are compared in Window 17 and Window 19, respectively.

The content of the "filter" program, Window 17, is shown in Figure 10. All traces are synchronized to the x-axis (the timing axis). The blue line is unfiltered EMG signal from channel 3, the "Bad data" channel, the green line is the IIR filtered EMG signal, and the red line is the Toco belt signal (channel 4). Notice the delay in the Toco belt signal compared to the EMG signal. Delays ranging from 20 to 35 seconds were computed in the data.

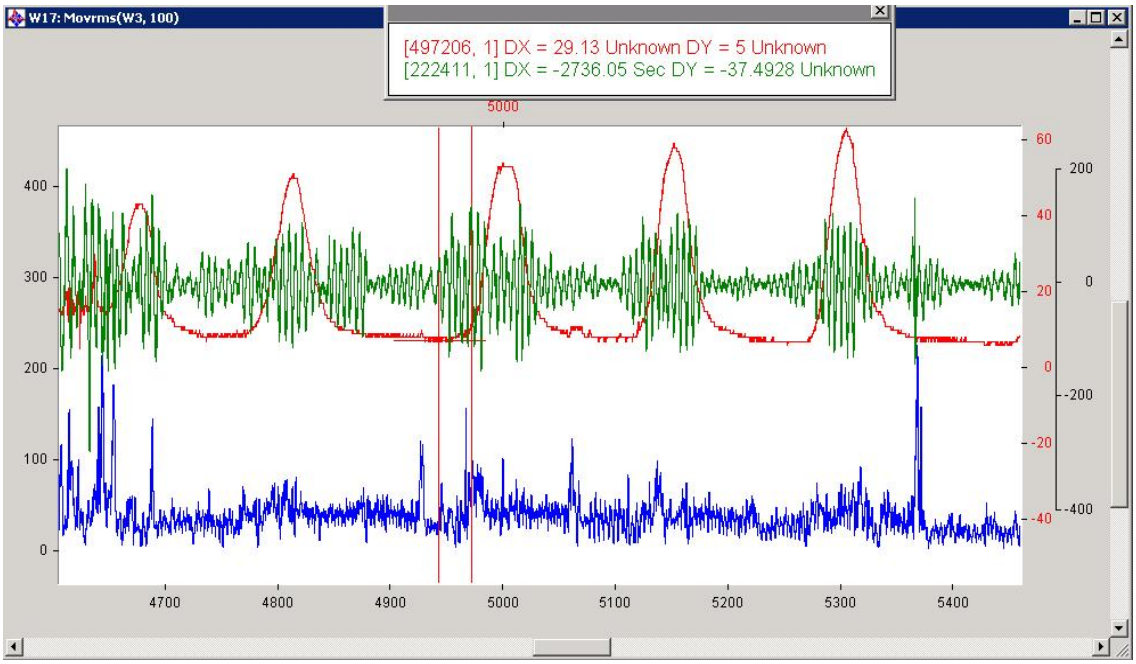

Figure 10. Window 17, moving RMS. The figure shows three traces synchronized in time. The blue trace is the unfiltered raw EMG signal from channel 3, the "Bad data" channel, the green trace is the IIR filtered EMG signal, and the red signal is the Toco belt signal (channel 4).

Spectral Analysis

With this approach, the spectral resolution of a 20 second window is 0.05 Hz. The energy in the frequency band between 0.25 and 0.40 Hz is summed and extracted in Window 8 (Figure 4) for every segment forming a matrix of frequency band energy versus time in seconds.

The last window (Window 19) was copied and exported to an EXCEL spreadsheet and is shown in Figure 11. The energy band trace is shown in blue and the Toco belt trace is shown in red. In most contractions there is a correspondence between the calculated trace and the Toco best trace.

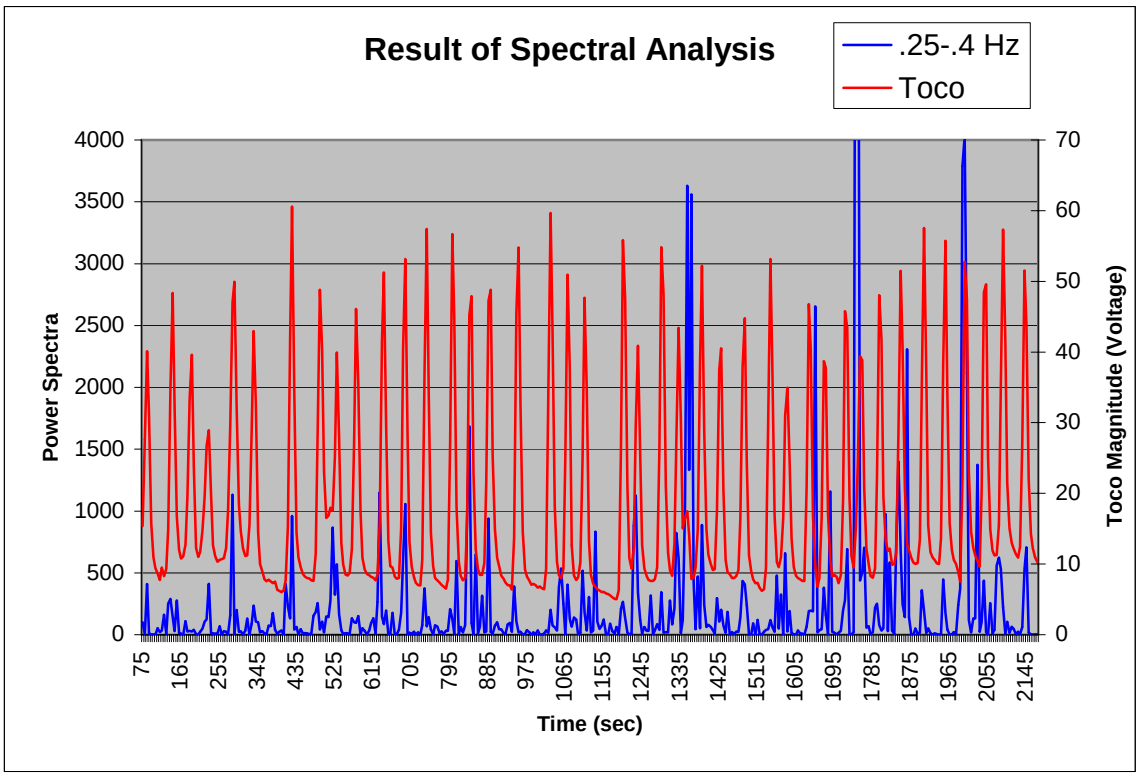

Figure 11. Excel summary of spectral analysis. The PSD energy band is shown in blue trace and the Toco belt trace is shown in red.

1/3 Octave Analysis

The results of 1/3 octave analysis are shown in Figure 12. Note that the uterine EMG signal follows the exact pattern as the Toco belt. Additionally, analysis using 60 second (Figure 13) and 90-second resolutions (Figure 14) were performed on the same EMG data file for comparison.

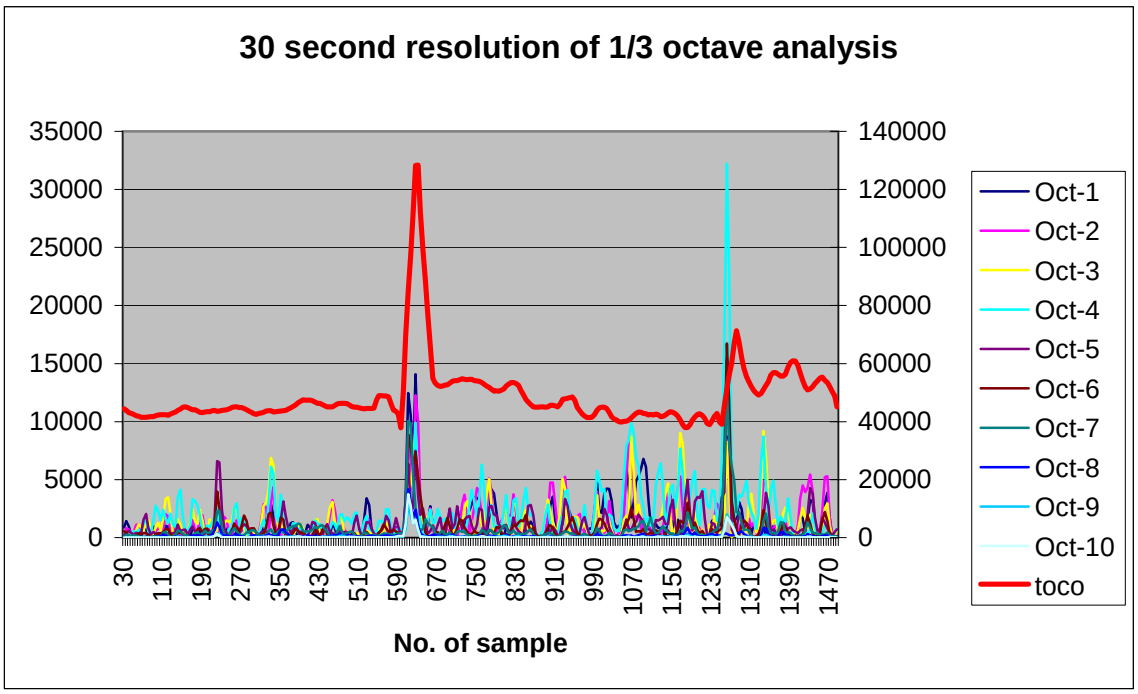

Figure 12. Excel plot of 30-second resolution of 1/3 octave analysis.

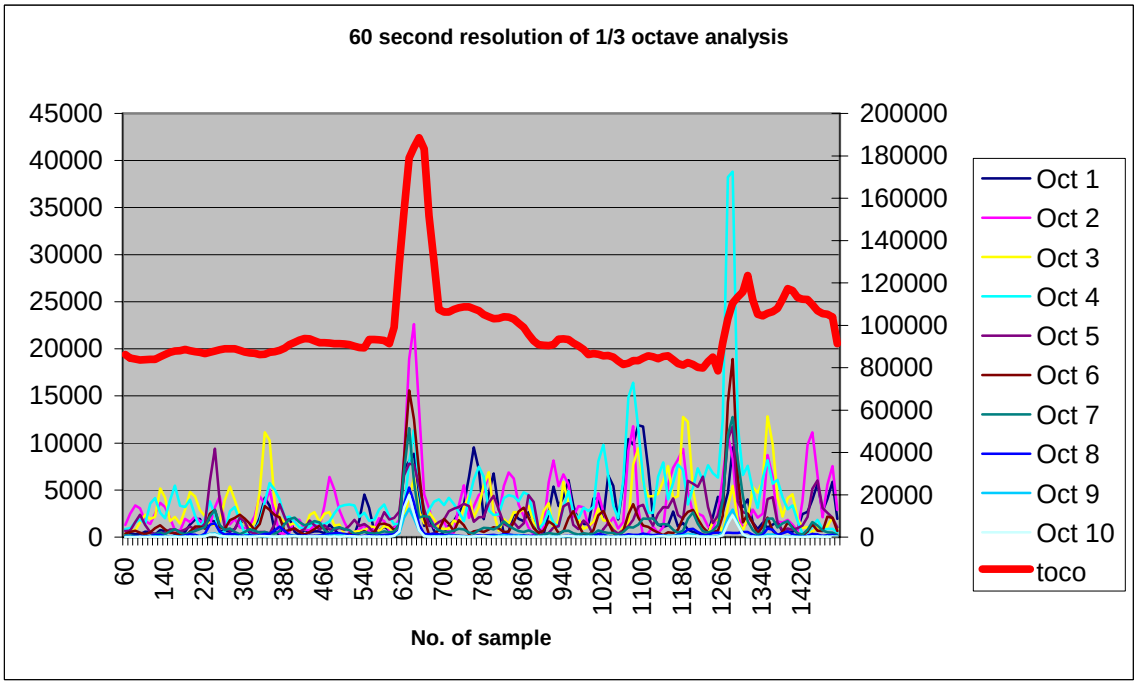

Figure 13. Excel plot of 60-second resolution of 1/3 octave analysis.

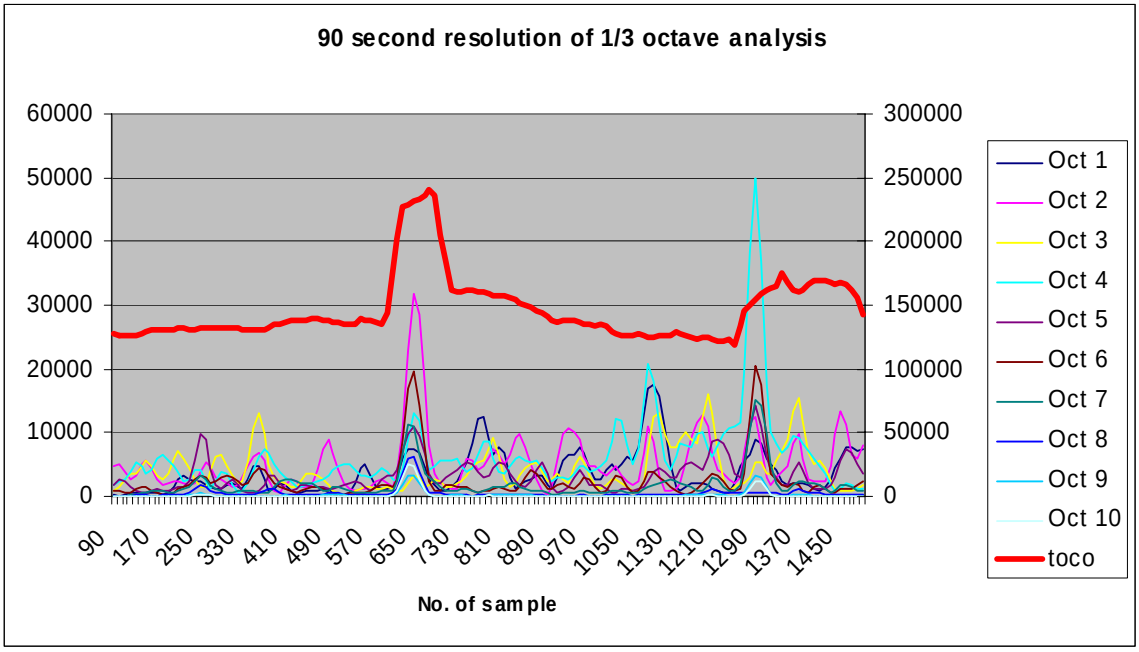

Figure 14. Excel plot of 90-second resolution of 1/3 octave analysis

Based on the results, it is noticed that the resultant traces of EMG signal of different resolutions are very similar. Hence, the 30-second resolution is selected for it has the smallest time delay. More plots of 1/3 octave analysis of different EMG data are included in the Appendix A.

Calculating Signal-to-Noise Ratio

Averages of 10 measures per channel within a record are introduced in Table 4 and the results of the paired t-test are shown in Table 5. Notice that the best average signal-to-noise ratio (SNR) in Table 4 is 6.434 for channel 2 of Record 3, however the average of the "Bad" channel of Record 5 (SNR=5.382) has a better signal-to-noise ratio than the "Good" channel (SNR=2.670). In general channel 2 has a mean SNR of 3.889

with a standard deviation of 2.289, whereas channel 3 has a mean SNR of 2.932 with a standard deviation of 1.639.

Table 4

Average signal to noise ratio

Record	Good Chan	Bad Chan	Difference
Averages	**SNR 2**	**SNR 3**	**Chan 2-3**
1	1.733	1.161	0.572
2	2.303	1.780	0.523
3	6.434	3.458	2.977
4	6.305	2.878	3.427
5	2.670	5.382	-2.712
Mean	3.889	2.932	0.957
Std Dev	2.289	1.639	2.448

Table 5 shows the result of paired t-test from the data in Table 4. The null hypothesis for the test is that there is no statistically difference between the SNR of channel 2 and the SNR of channel 3. The alternate hypothesis is that there are significant differences between the two SNRs. With the significance level set at 5% ($\alpha = 0.05$), the two-sided test failed to show that there is no difference; hence, the null hypothesis is rejected and the alternate hypothesis is accepted. Therefore, it is concluded that there is a significance difference between the SNR of channel 2 and the SNR of channel 3.

Table 5

Paired t-test

t-Test: Paired Two Sample for Means		
SNR Chan 2 = SNR Chan 3	$\alpha =$ **0.05**	
	Variable 1	***Variable 2***
Mean	3.889006062	2.931643031
Variance	5.241064629	2.686172665
Observations	5	5
Pearson Correlation	0.257587206	
Hypothesized Mean Difference	0	
df	4	
t Stat	0.874368599	
P(T<=t) one-tail	0.215637203	
t Critical one-tail	2.131846486	
P(T<=t) two-tail	**0.431274405**	**Reject**
t Critical two-tail	2.776450856	

Discussion

Overall 15 data files were randomly selected for further analysis using frequency analysis, filter and 1/3 octave analysis. Among these selected files, 7 were considered bad data files due to the fact that the Toco signal (reference signal) was bad, the uterine EMG signal was bad or both of them were bad. Hence the uterine contraction peaks in the signal could not be recognized. Figure 15 shows an example of a bad data file in which there are no distinguished uterine contraction signals in either the Toco belt or

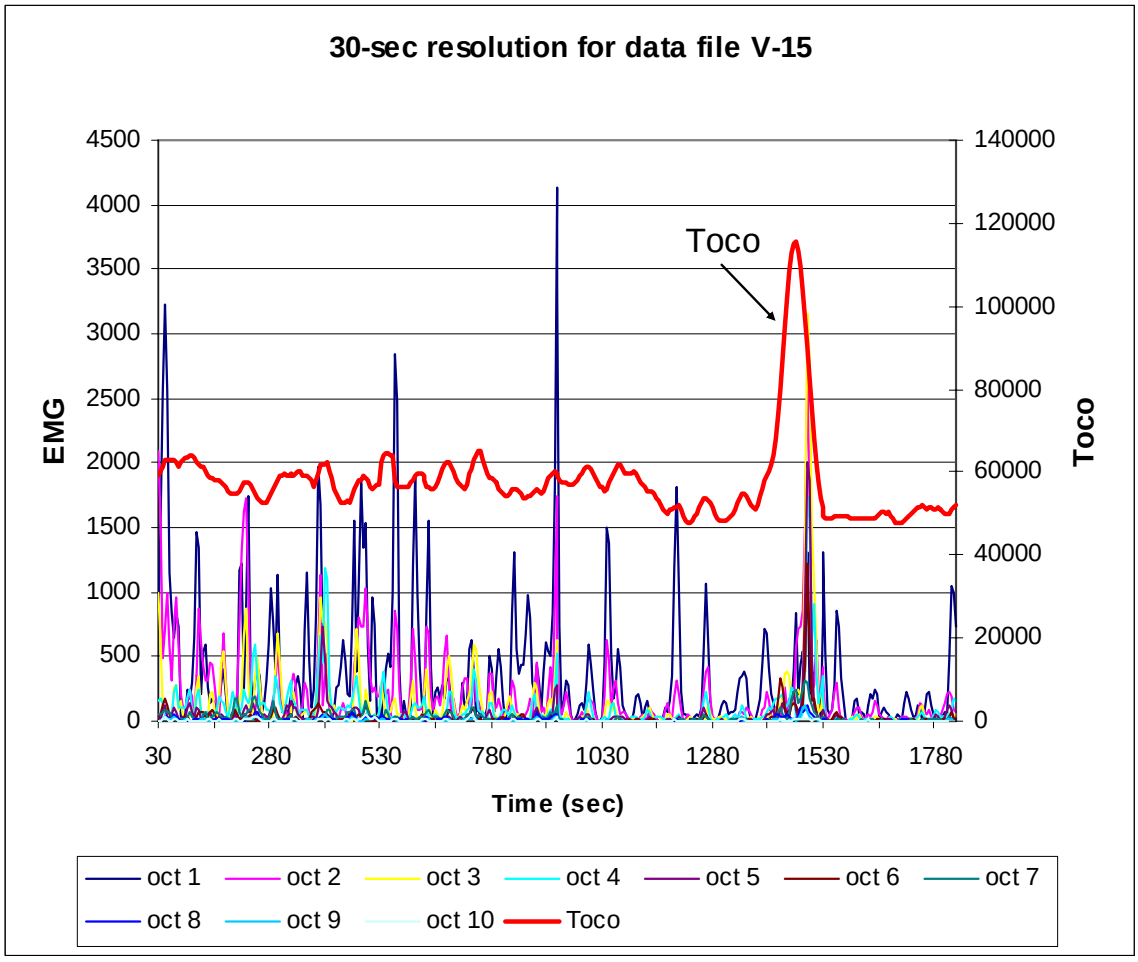

Figure 15. An example of unrecognizable uterine contractions files.

EMG signal. Although there is one peak energy shown at around 1530-second, whether it is motion artifact or true uterine contraction needs an expert to validate.

For those good files (N=8), the number of correct detection (uterine contractions detected by both the Toco belt and the EMG) and the number of missed detection (uterine contractions detected by the Toco belt but not the EMG) are measured. In Figure 16, “B” is the uterine contraction signal which corresponds to the Toco signal “A”;

hence, that is a correct detection. "C" is the signal peak detected by electromyogram but there is no correspondence signal recorded by tocodynamometer, so it is false detection (uterine contractions detected by the EMG but not the Toco belt). An example of missed detection is marked "D" as there is no peak energy signal shows in the EMG signal whereas Toco belt shows a contraction.

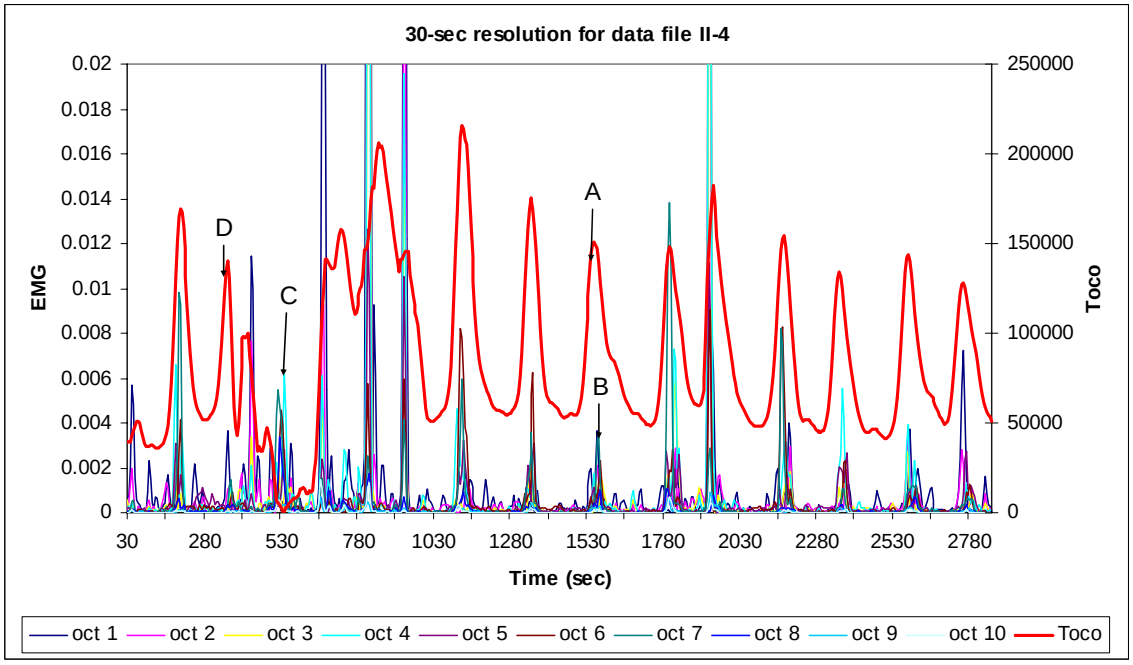

Figure 16. An example of good data files, and the categorization of correct detection, missed detection and false detection.

"Good" data files (N=8) are analyzed using 1/3 octave analysis, frequency analysis and filter (Butterworth, Bandstop). The comparison of the probability of correct detection (uterine contractions detected by both the Toco belt and the EMG) and missed detection (uterine contractions detected by the Toco belt but not the EMG) are shown in Figures 17 and 18, respectively. Figure 17 shows that the 1/3 octave analysis has the highest correct percentage (about 78.5 %) and frequency analysis has the lowest correct

percentage, less than 76%. Filter application has a fair performance, with about 77.8% correct detection and about 22% of missed detection.

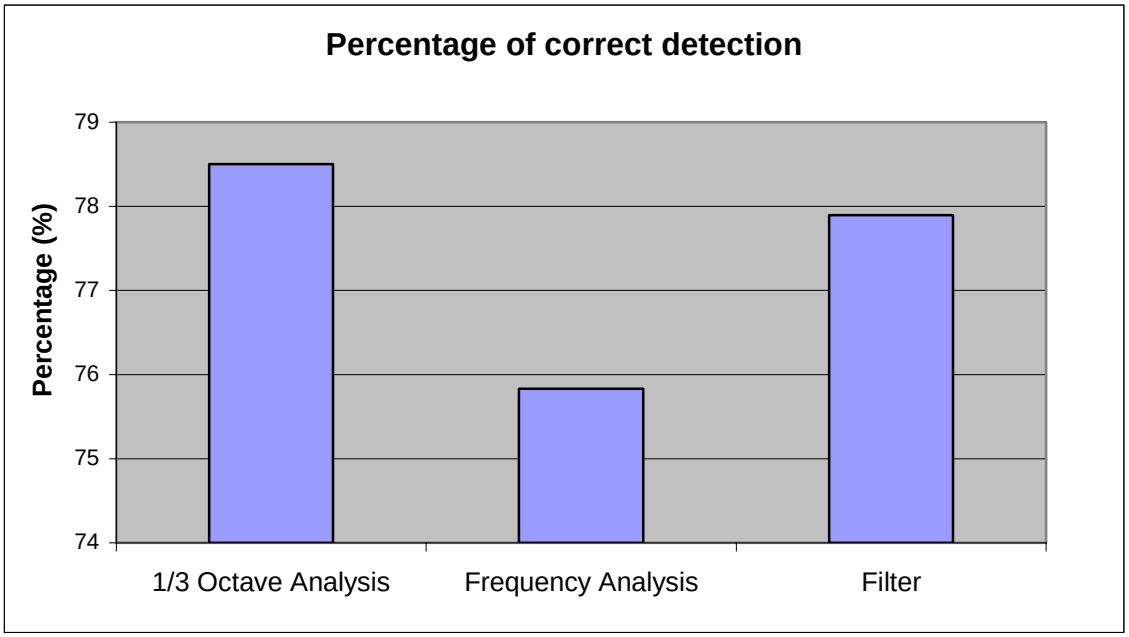

Figure 17. Percentage of correct detection by EMG with various methods.

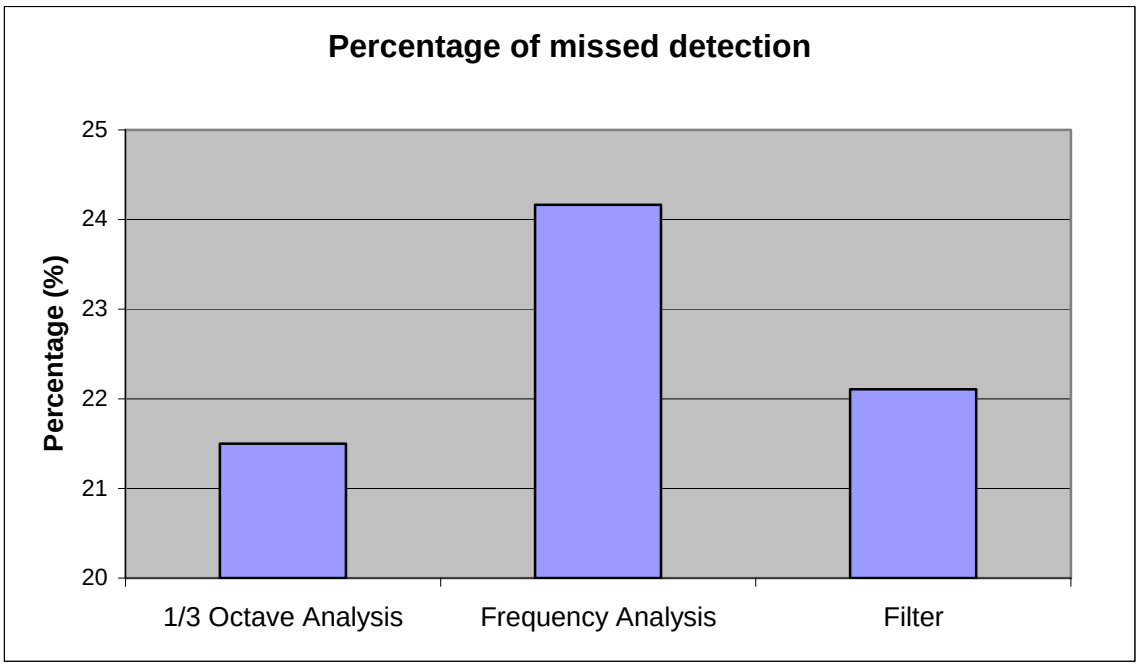

Figure 18. Percentage of missed detection by EMG with various methods.

The number of false detection (uterine contractions detected by the EMG but not the Toco belt) was counted and the result is shown in Figure 19.

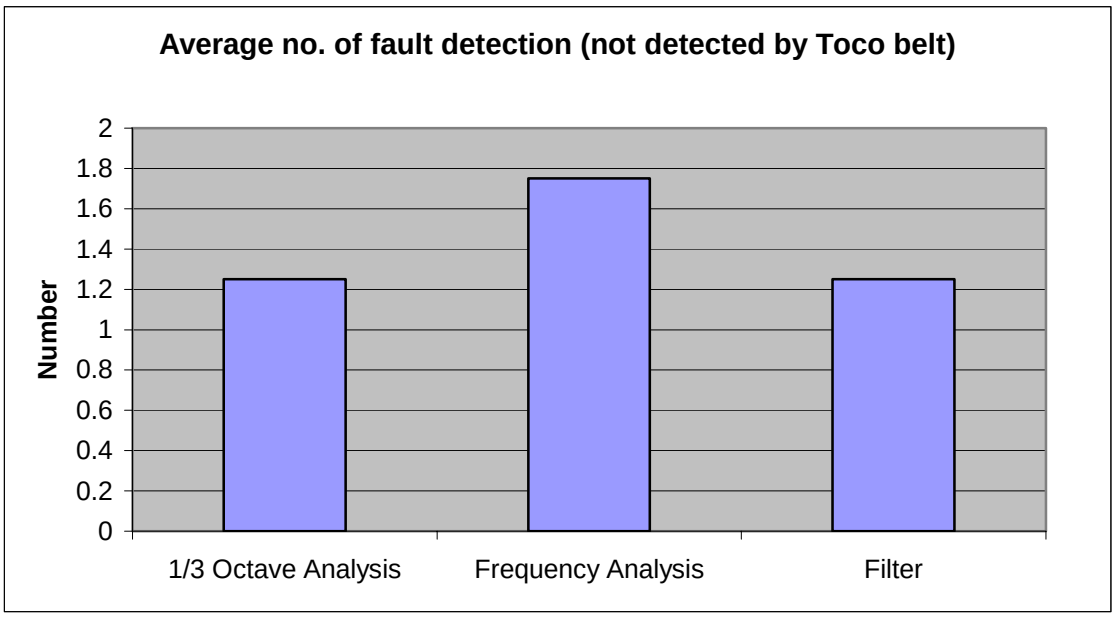

Figure 19. Average number of false detections (not detected by Toco belt). The values (Y-values) in the figure represent the average of 8 data files.

In addition to analyzed ten 1/3-octave bands all together with Toco belt, the average value and the maximum value across these ten 1/3-octave bands' power spectral density function are taken, and plot each value with Toco signal in Figures 20 and 21, respectively. The results are not much difference from what we have in Figure 16, a similar pattern of energy distribution with uterine contractions correspond to the Toco signal. Other possible way to analyze these 1/3-octave bands is to calculate their RMS values and plot them together, and/or separately with the Toco signal.

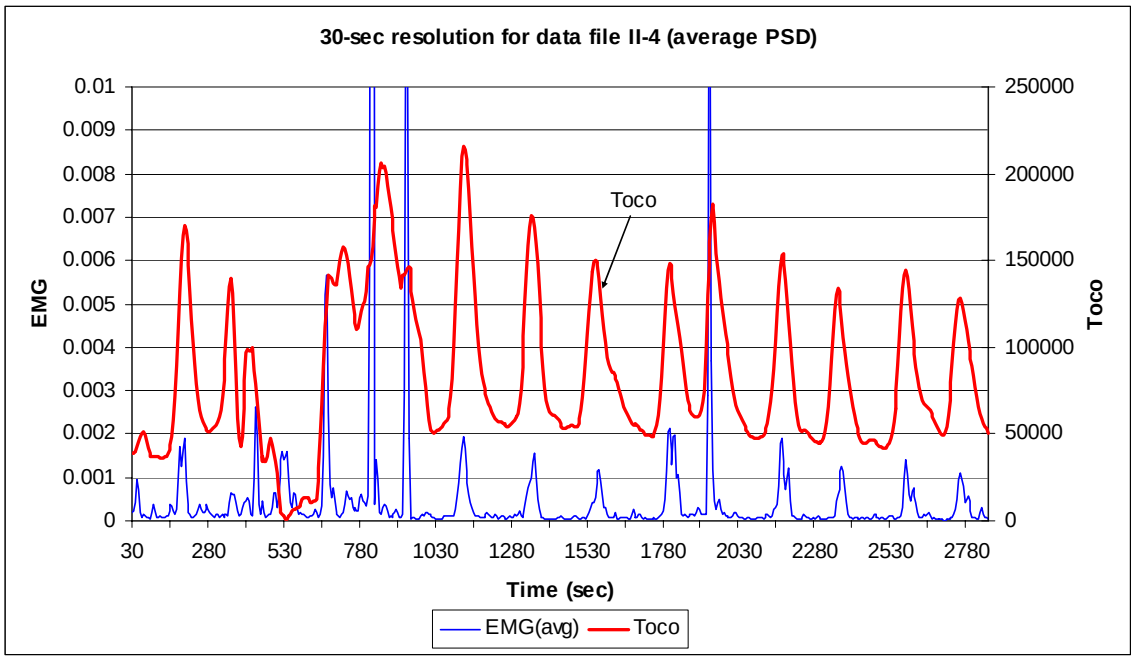

Figure 20. A plot of average PSD value of EMG with Toco belt signal.

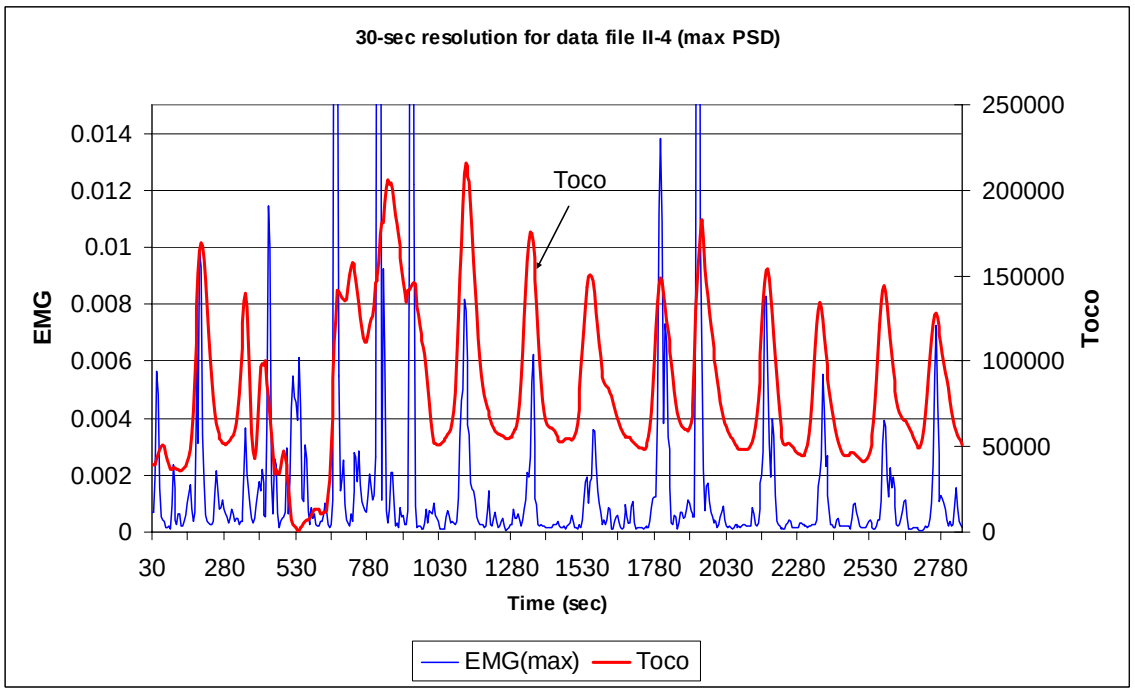

Figure 21. A plot of maximum PSD value of EMG with Toco belt signal.

CONCLUSIONS

The primary objective of this study was to remove or, at least, reduce the noise in the noisy uterine EMG recordings, which at their present noise level render the data unusable. A secondary goal was to evaluate and develop a very narrow band digital filter in order to increase the signal-to-noise ratio. The last objective was to extract EMG features (parameters) from the data so as to enhance detection of the uterine EMG signals.

From the results the following conclusions were drawn:

1. The signal-to-noise ratio (SNR) was increased from 1.1613 to 1.5327 after filtering with an IIR Butterworth stopband filter; however it should be noticed that the SNR varies quite a bit with a standard deviation of 0.9575 and variance of 0.9167 in channels referred as “Good”.
2. The frequency analysis via a spectral band between 0.25 and 0.4 Hz shows promise of matching the Toco belt.
3. The 1/3 octave analysis gives the highest correct detection (uterine contractions detected by both the Toco belt and the EMG) percentage (78.5%); however, there is a tradeoff. Even though the 1/3 octal gave the best results there is about a 30-seconds time delay (3000 data points) in acquiring and processing the EMG data. Nevertheless the 30 second delay approximated the delay from the onset of uterine EMG to the onset

of the tocodynamometer signal; thus almost matching the delay from the output of the Toco belt.

4. Because of the lack of Expert scoring of the onset of “True EMG labor contractions”, the probability of correctly detecting “true” uterine contractions could not be validated.

RECOMMENDATIONS

Since lack of Expert scoring of the onset of “True EMG labor contractions”, it is recommended to add two more channels of recording. Of these additional channels, one is for the physician to record the onset of true labor contractions, and another is for the subject to trigger the signal when labor contraction occurs and release when it is over, throughout the whole recording process. Identifying the onset and duration of true contractions will help researchers to distinguish what a true contraction is versus a false contraction. Future work such as neural network could be designed and trained to automate the identification process.

REFERENCES

[1] U.S. Preventive Services Task Force, *Guide to clinical preventive services: An assessment of the effectiveness of 169 interventions*, Baltimore: Williams & Wilkins, 1989.

[2] S.J. Ventura, J.A. Martin, S.C. Curtin and T.H. Matthews, "Report of final natality statistics," *Monthly Vital Stat Rep*, vol. 45, p.12, 1997.

[3] E.R. Brown, M. Epstein, "Immediate consequences of preterm birth" in *Preterm birth: Causes, prevention, and management*, F. Fuchs and P.G. Stubblefield, Eds. New York: Macmillan Publishing, 1984, pp. 323–354.

[4] R.L. Goldenberg, S.P. Cliver, J. Bronstein, G.R. Cutter, W.W. Andrews and S.T. Mennemeyer, "Bed rest in pregnancy," *Obstet Gynecol*, vol. 84, pp. 131-136, 1994.

[5] R.E. Garfield, H. Maul, W. Maner, C. Fittkow, G. Olson, L. Shi, and G. R. Saade, "Uterine electromyography and light-induced fluorescence in the management of term and preterm labor," *Journal of Society for Gynecologic Investigation*, vol. 9, pp. 265-275, 2002.

[6] R.J. Wapner, D.B. Cotton, R. Artal, R.J. Librizzi and M.G. Ross, "A randomized multicenter trial assessing a home uterine activity monitoring device used in the absence of daily nursing contact," *Am J Obstet Gynecol*, vol. 172, pp. 1026-1034, 1995.

[7] The Collaborative Home Uterine Monitoring Study Group, "A multicenter randomized controlled trial of home uterine monitoring: Active vs sham device," *Am J Obstet Gynecol*, vol. 173, pp. 1117-1120, 1995.

[8] H.F. Andersen, C.E. Nugent, S.D. Wanty and R.H. Hayashi, "Prediction of risk for preterm delivery by ultrasonographic measurement of cervical length," *Am J Obstet Gynecol*, vol. 163, pp. 859-867, 1990.

[9] E.R. Guzman, C. Houlihan and A. Vintzileos, "Sonography and transfundal pressure in the evaluation of the cervix during pregnancy," *Obstet Gynecol Survey*, vol. 50, pp. 395-403, 1995.

[10] T.K.H. Chung, C.J. Haines, D. Kong, W.K. Woo and M.S. Rogers, "Transvaginal sonography in the diagnosis and management of cervical incompetence," *Gynecol Obstet Invest*, vol. 36, pp. 59-61, 1993.

[11] J.D. Iams, R.L. Goldenberg and P.J. Meis, "The length of the cervix and the risk of spontaneous premature delivery," *N Engl J Med*, vol. 334, pp. 567-572, 1996.

[12] C.M. Cook and D.A. Ellwood, "A longitudinal study of the cervix in pregnancy using transvaginal ultrasound," *Br J Obstet Gynecol*, vol. 103, pp. 16-18, 1996.

[13] J.D. Iams, J. Paraskos, M.B. Landon, J.N. Teteris and F.F. Johnson, "Cervical sonography in preterm labor," *Obstet Gynecol*, vol. 84, pp. 40-46, 1994.

[14] C.J. Lockwood, R. Wein and R. Lapinksi, "The presence of cervical and vaginal fetal fibronectin predicts preterm delivery in an inner-city obstetric population," *Am J Obstet Gynecol*, vol. 169, pp. 798-804, 1993.

[15] M.P. Nageotte, D. Casal and A.E. Senyei, “Fetal fibronectic in patients at increased risk for premature birth,” *Am J Obstet Gynecol*, col. 170, pp. 20-25, 1994.

[16] C.J. Lockwood, R.D. Moscarelli, R. Wein, L Lynch, R.H. Lapinski and A. Ghidini, “Low concentrations of vaginal fetal fibronectin as a predictor of deliveries occurring after 41 weeks,” *Am J Obstet Gynecol*, vol. 171, pp. 1-4, 1994.

[17] P. Hellemans, J. Gerris and P. Verdonk, “Fetal fibronectin detection for prediction of preterm birth in low risk women,” *Br J Obstet Gynecol*, vol. 102, pp. 207-212, 1995.

[18] J.D. Iams, D. Casal and J.A. McGregor, “Fetal fibronectin improves the accuracy of diagnosis of preterm labor,” *Am J Obstet Gynecol*, vol. 173, pp. 141-145, 1995.

[19] J.A. McGregor, G.M. Jackson and G.C. Lachelin, “Salivary estriol as risk assessment for preterm labor: A prospective trial,” *Am J Obstet Gynecol*, vol. 173, pp. 1337-1342, 1995.

[20] R.L. Copper, R.L. Goldenberg, M.B. Dubard, J.C. Hauth and G.R. Cutter, “Cervical examination and tocodynamometry at 28 weeks’ gestation: Prediction of spontaneous preterm birth,” *Am J Obstet Gynecol*, vol. 172, pp. 666-671, 1995.

[21] C. Buhimschi and R.E. Garfield, “Uterine contractility as assessed by abdominal surface recording of electromyographic activity in rats during pregnancy,” *Am J Obstet Gynecol*, vol. 174, pp. 744-753, 1996.

[22] W.J. Hueston, “Preterm contractions in community settings. II. Predicting preterm birth in women with preterm contractions,” *Obstet Gynecol*, vol. 92, pp. 43-46, 1998.

[23] D. Devedeux, C. Marque, S. Mansour, G. Germain and J. Duchene, "Uterine electromyography: A critical review,"*Am J Obstet Gynecol*, vol. 169, pp. 1636-1653, 1993.

[24] M. Pajntar, E. Roskar and D. Rudel, "Electromyographic observation of the human cervix during labor," *Am J Obstet Gynecol*, vol. 156, pp. 691-697, 1987.

[25] C. Buhimschi, M.B. Boyle and R.E. Garfield, "Electrical activity of the human uterus during pregnancy as recorded from the abdominal surface," *Obstet Gynecol*, vol. 90, pp. 102-111, 1997.

[26] A.I. Csapo, "Force of labor," in *Principles and practice in obstetrics and perinatology*, L. Iffy and H.A. Kamientzky, Eds. New York: John Wiley, 1981, pp. 761-799.

[27] G.M.J.A. Wolfs and M. Van Leeuwen, "Electromyographic observations on the human uterus during labour," *Acta Obstet Gynecol Scan Suppl*, vol. 90, pp. 1-61, 1979.

[28] R. Harding, E.R. Poore, A. Bailey, G.D. Thorburn, C.A.M Jansen and P.W. Nathanielsz, "Electromyographic activity of the nonpregnant and pregnant sheep uterus," *Am J Obstet Gynecol*, vol. 142, pp. 448-451, 1982.

[29] H. Demianczuk, M.E. Towell and R.E. Garfield, "Myometrial electrophysiologic activity and gap junctions in the pregnant rabbit," *Am J Obstet Gynecol*, vol. 149, pp. 485-491, 1984.

[30] A. Verhoeff, "Modulation of spontaneous myometrial activity in chronically instrumented ovariectomized sheep," in *Myometrial contractility and gap*

junctions: an experimental study in chronically instrumented ewes, A. Verhoeff, Ed. Alblasserdam: Offsetdrukkerij Kanters BV, pp. 40-53, 1985.

[31] P.W. Nathanielsz, Z. Binienda, J. Wimsatt, J.P. Figueroa and A. Massmann, "Patterns of myometrial activity and their regulation in the pregnant monkey," in *The onset of labor: cellular integrative mechanisms*, Ithaca, New York: Perinatology Press, 1988, pp. 359-383.

[32] R.E. Garfield, M.G. Blennerhassett and S.M. Miller, "Control of myometrial contractility: Role and regulation of gap junctions," *Oxford reviews of reproductive biology*, Oxford: Oxford University Press, pp. 436-490, 1988.

[33] J.M. Marshall, "Regulation of activity in uterine smooth muscle," *Physiol Rev*, vol. 42, pp. 213-227, 1982.

[34] H. Kuriyama, "Recent studies of the electrophysiology of the uterus," in *Progesterone and the defence mechanism of pregnancy*, Ciba Foundation Study Group, Boston: Little Brown, vol 9. pp. 51–70, 1961.

[35] A.I. Csapo, "Smooth muscle as a contractile unit," *Physiol Rev*, vol. 42, pp. 7-33, 1962.

[36] H. Okawa, "Electrical and mechanical interaction between the muscle layers of rat uterus and different sensitivities to oxytocin," *Bull Yamaguchi Med School*, vol. 22, pp. 197-210, 1975.

[37] H. Kuriyama and H. Suzuki, "Changes in electrical properties of rat myometrium during gestation and following hormonal treatments," *J Physiol (Lond)*, vol. 260, pp. 315-333, 1976.

[38] S. Kanda and H. Kuriyama, “Specific features of smooth muscle cells recorded from the placental region of the myometrium of pregnant rats,” *J Physiol (Lond)*, vol 299, pp. 127-144, 1980.

[39] T. Osa and T. Fujino, “Electrophysiological comparison between the longitudinal and circular muscles of the rat uterus during the estrous cycle and pregnancy,” *Jpn J Physiol*, vol. 23, pp. 197-209, 1978.

[40] T. Osa, T. Ogasawara and S. Kato, “Effects of magnesium, oxytocin and prostaglandin F2 on the generation and propagation of excitation in the longitudinal muscle of rat myometrium during late pregnancy,” *Jpn J Physiol*, vol. 33, pp. 51-67, 1983.

[41] B. Bengtsson, E.M.H. Chow and J.M. Marshall, “Activity of circular muscle of rat uterus at different times in pregnancy,” *Am J Physiol*, vol. 246, pp. C216-C223, 1984.

[42] T. Kawarabayashi and J.M. Marshall, “Factors influencing circular muscle activity in the pregnant rat uterus,” *Biol Reprod*, vol. 24, pp. 373-379, 1981.

[43] G.F. Anderson, T. Kawarabayashi and J.M. Marshall, “Effect of indomethacin and aspirin on uterine activity in pregnant rats: Comparison of circular and longitudinal muscle,” *Biol Reprod*, vol. 24, pp. 359-372, 1981.

[44] J.M. Marshall, “Effects of estrogen and progesterone on single uterine muscle fibers in the rat,” *Am J Physiol*, vol. 197, pp. 935-942, 1959.

[45] M.B. Honnebier, R.A. Wentworth, J.P. Figueroa and P.W. Nathanielsz, “Temporal structuring of delivery in the absence of a photoperiod: Preparturient myometrial

activity of the rhesus monkey is related to maternal body temperature and depends on the maternal circadian system," *Biol Reprod*, vol. 45, pp. 617-625, 1991.

[46] M.A.M. Taverne and J. Scheerboom, "Myometrial electrical activity during pregnancy and parturition in the pigmy goat," *Res Vet Sci*, vol. 38, pp. 120-123, 1985.

[47] C.A. Ducsay and C.M. McNutt, "Circadian uterine activity in the pregnant rhesus macaque: Do prostaglandins play a role?," *Biol Reprod*, vol. 40, pp. 988-993, 1989.

[48] P.W. Nathanielsz, A. Bayley, E.R. Poore, G.D. Thorburn and R. Harding, "The relationship between myometrial activity and sleep state and breathing in fetal sheep throughout the last third of gestation," *Am J Obstet Gynecol*, vol. 138, pp. 653-659, 1980.

[49] C. Sureau, J. Chavinie and M. Cannon, "L'electrophysiologie uterine," *Bull Fed Soc Gynecol Obstet*, vol. 17, pp. 79-140, 1965.

[50] A. Verhoeff, R.E. Garfield, J. Ramondt and H.C. Wallenburg, "Myometrial activity related to gap junction area in periparturient and in ovariectomized estrogen treated sheep," *Acta Physiol Hung*, vol. 67, pp. 117-129, 1986.

[51] J.P. Figueroa, S. Mahan, E.R. Poore and P.W. Nathanielsz, "Characteristics and analysis of uterine electromyographic activity in the pregnant sheep," *Am J Obstet Gynecol*, vol. 151, pp. 524-531, 1985.

[52] C. Sureau, "Etude de l'activite electrique de l'uterus au cours du travail," *Gynecol Obstet*, vol. 555, pp. 153-175, 1956.

[53] G.M.J.A. Wolfs and H. Rottinghuis, “Electrical and mechanical activity of the human uterus during labour,” *Arch Gynaekol*, vol. 208, pp. 373-385, 1970.

[54] P. Lopes, G. Germain, G. Breart, S. Reinatin, R. Le Houezec and C Sureau, “Electromyographical study of uterine activity in the human during labor induced by prostaglandin,” *Gynecol Obstet Invest*, vol. 17, pp. 96-105, 1984.

[55] A. Csapo and H. Takeda, “Electrical activity of the parturient human uterus,” *Nature*, vol. 200, p. 68, 1963.

[56] A. Csapo and J. Sauvage, “The evolution of uterine activity during human pregnancy,” *Acta Obstet Gynecol Scand*, vol. 47. pp. 181-212, 1968.

[57] C. Buhimschi, M.B. Boyle and R.E. Garfield, “Electrical activity of the human uterus during pregnancy as recorded from the abdominal surface,” *Obstet Gynecol*, vol. 90, pp. 102-111, 1997.

[58] C. Buhimschi, M.B. Boyle, G.R. Saade and R.E. Garfield, “Uterine activity during pregnancy and labor assessed by simultaneous recordings from the myometrium and abdominal surface in the rat,” *Am J Obstet Gynecol*, vol. 178, pp. 811-822, 1998.

[59] J. Duchêne, D. Devedeux, S. Mansour and C. Marque, “Analyzing uterine EMG: Tracking instantaneous burst frequency,” *IEEE Eng Med Biol*, vol. 14, pp. 125-132, 1995.

[60] C. Marque, J. Duchêne, S. Lectercq, G. Panczer and J. Chaumont, “Uterine EMG processing for obstetrical monitoring,” *IEEE Trans Biomed Eng*, vol. 33, pp. 1182-1187, 1986.

[61] C. Lessard, “Recovering the uterine Electromyographic Signals (EMG) from noisy abdominal surface electrodes,” unpublished paper, pp. 3-4, 2003.

[62] “Analyze signals octave by octave”, (2003, Sept. 15). www.e-insite.net [online].

APPENDIX A

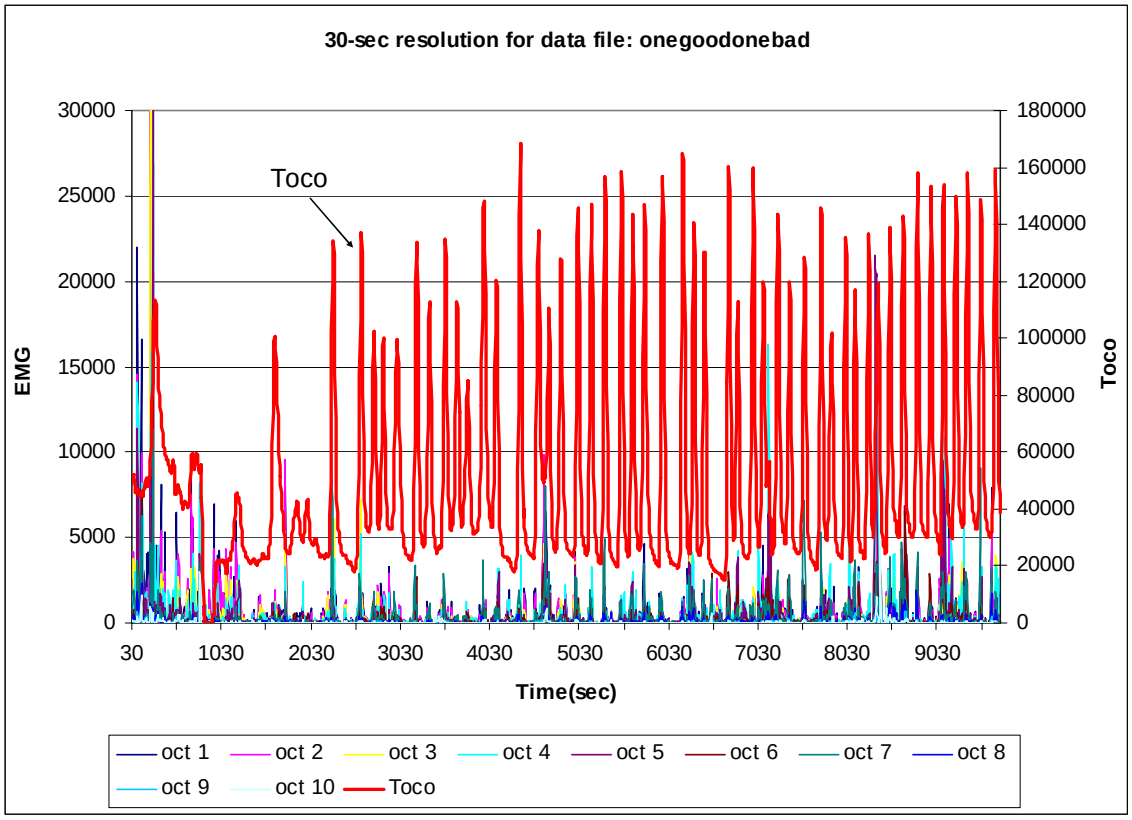

Figure A1. Excel plot of 30-second resolution of 1/3 octave analysis for data file: onegoodonebad.

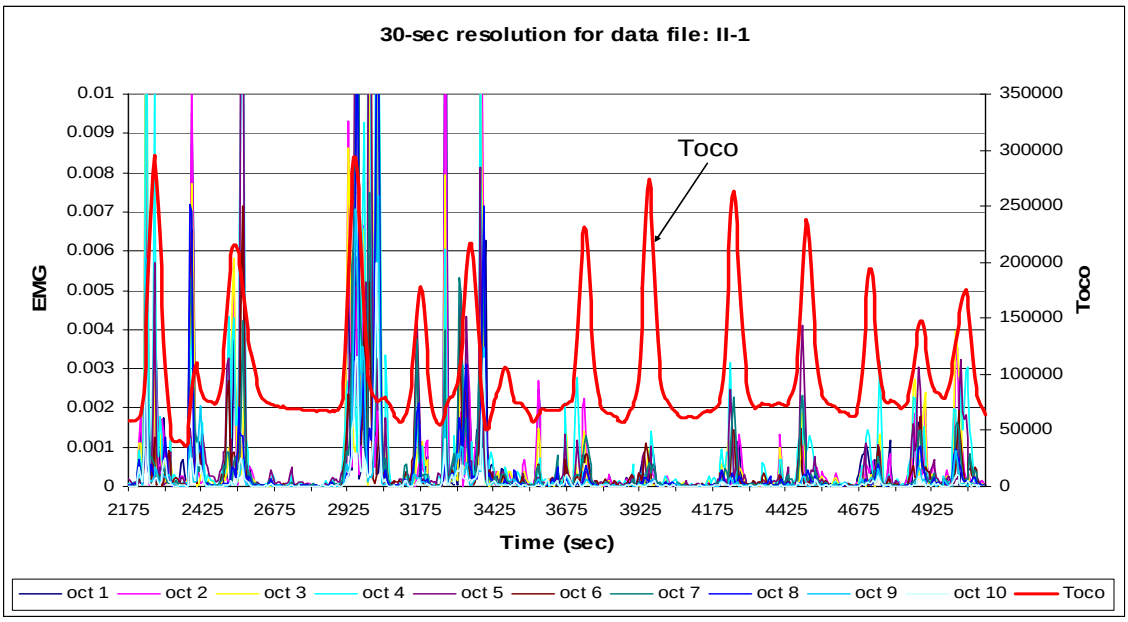

Figure A2. Excel plot of 30-second resolution of 1/3 octave analysis for data file: II-1.

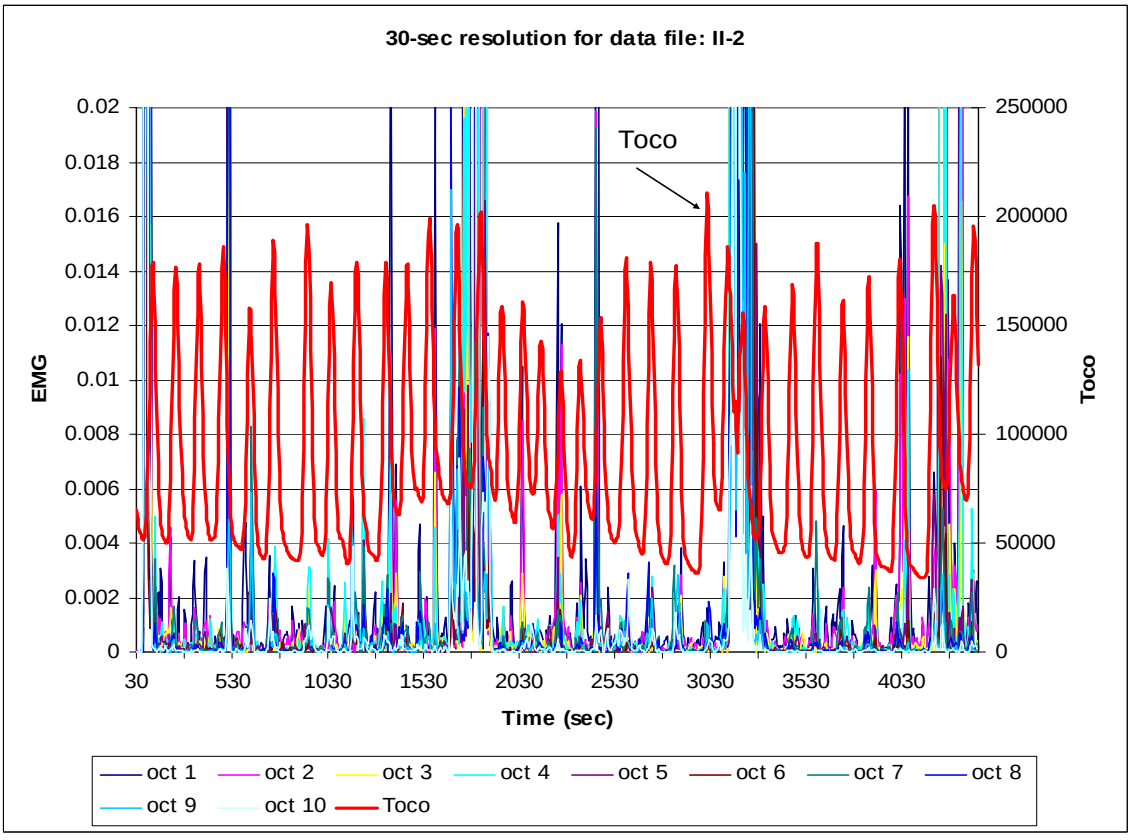

Figure A3. Excel plot of 30-second resolution of 1/3 octave analysis for data file: II-2.

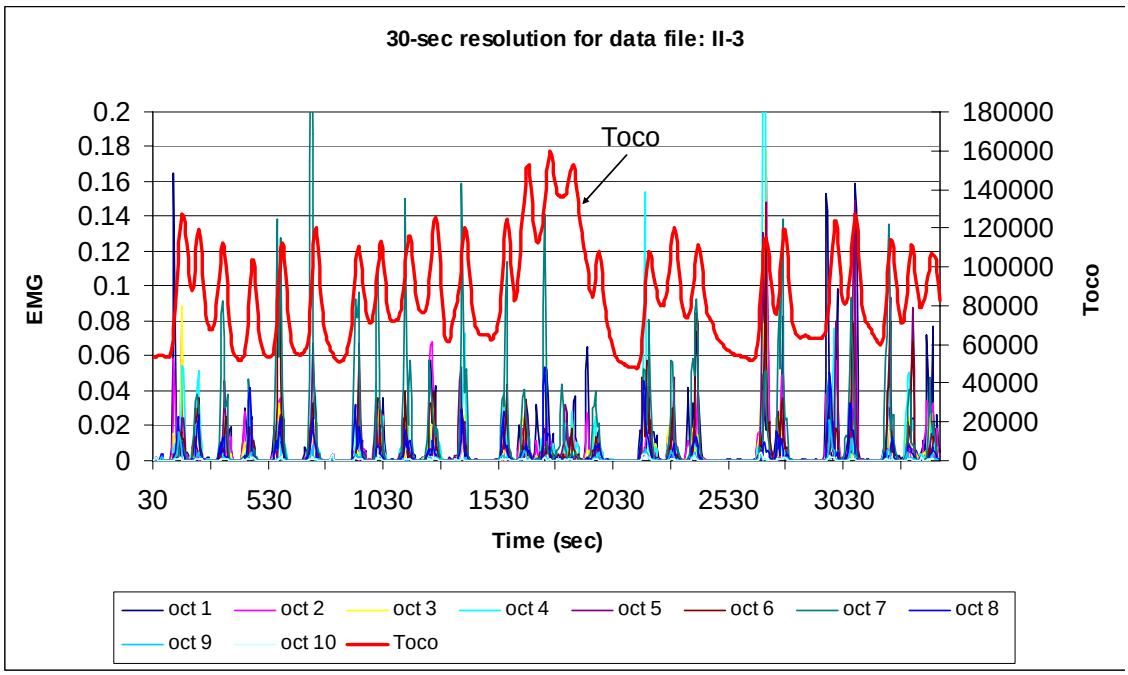

Figure A4. Excel plot of 30-second resolution of 1/3 octave analysis for data file II-3.

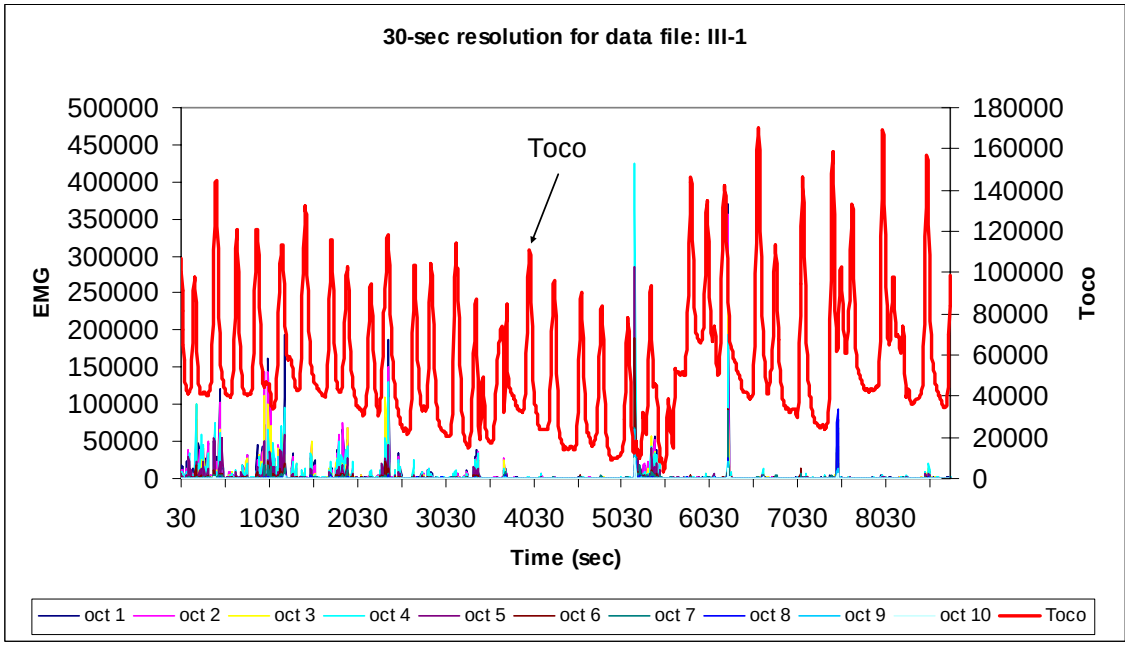

Figure A5. Excel plot of 30-second resolution of 1/3 octave analysis for data file: III-1.

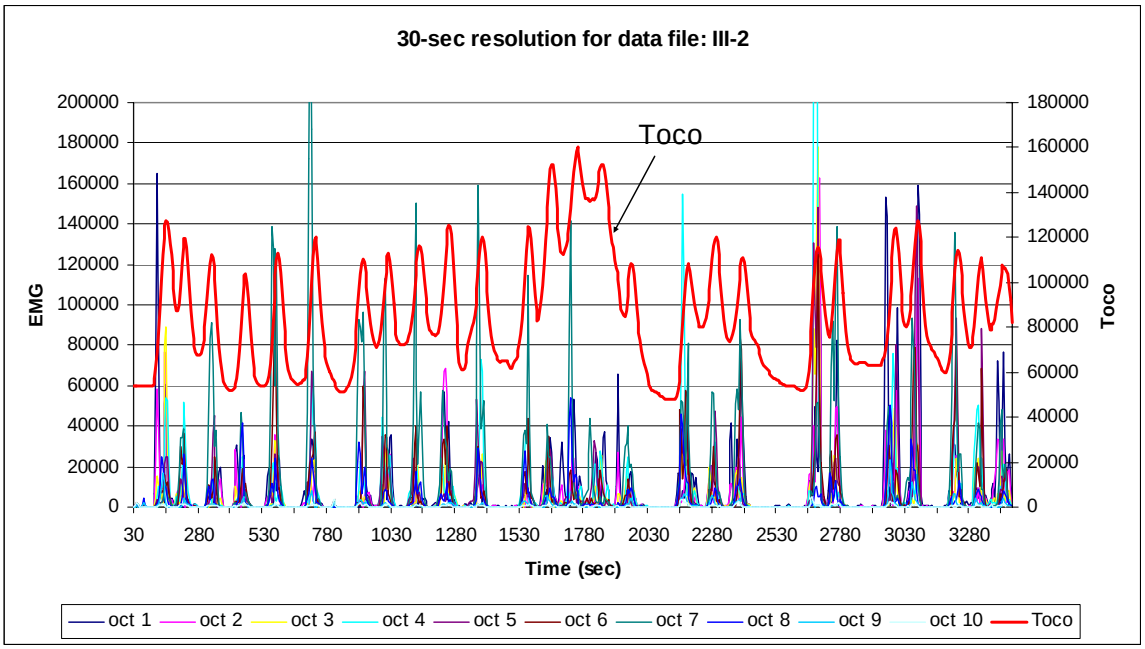

Figure A6. Excel plot of 30-second resolution of 1/3 octave analysis for data file: III-2.

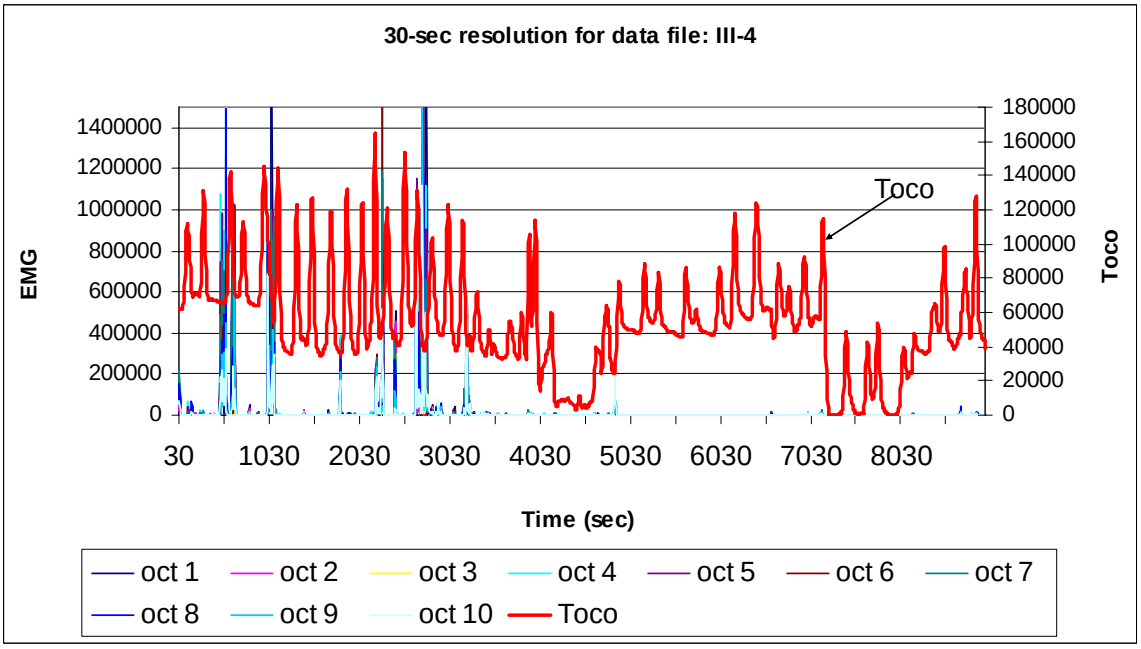

Figure A7. Excel plot of 30-second resolution of 1/3 octave analysis for data file: III-4.

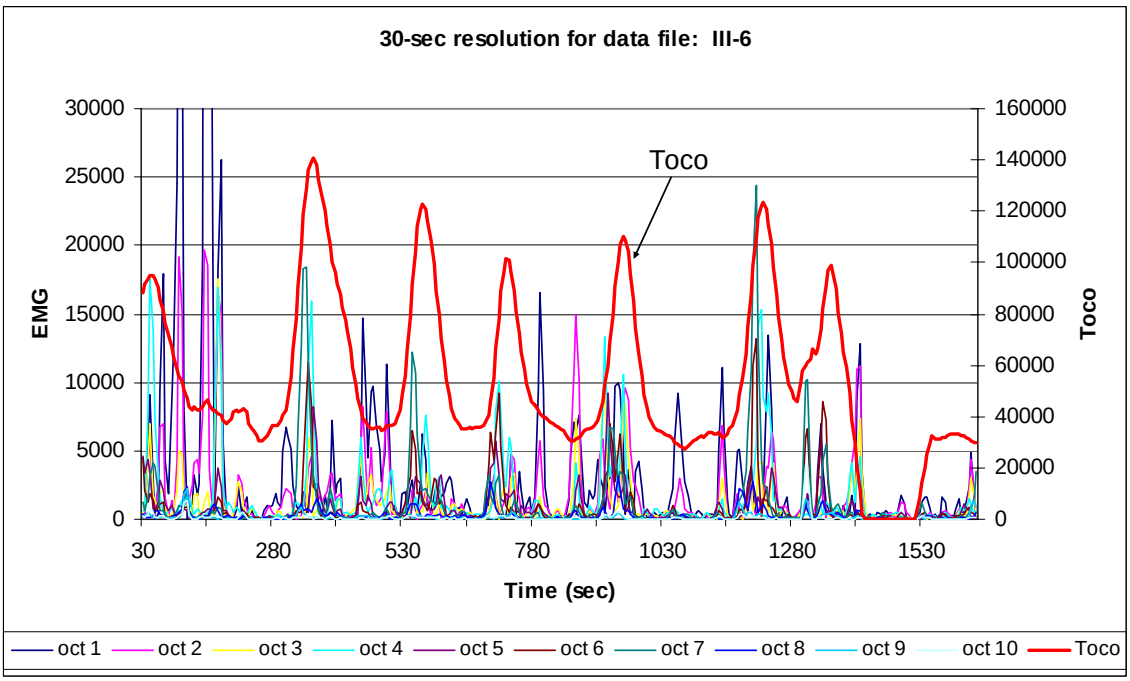

Figure A8. Excel plot of 30-second resolution of 1/3 octave analysis for data file: III-6.

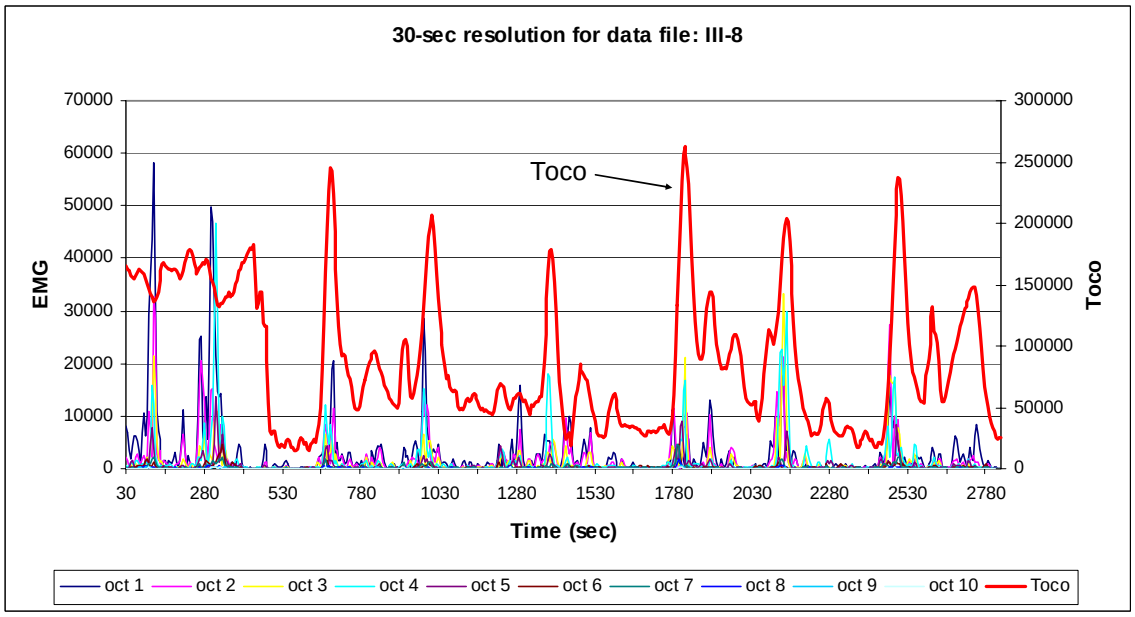

Figure A9. Excel plot of 30-second resolution of 1/3 octave analysis for data file: III-8.

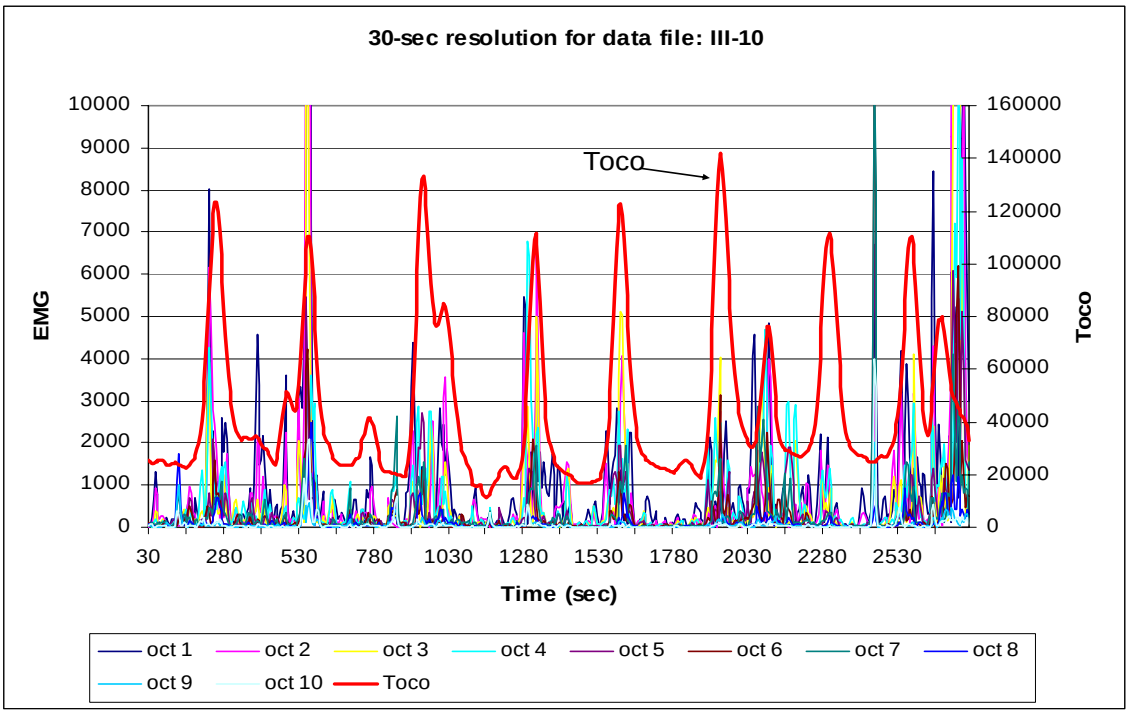

Figure A10. Excel plot of 30-second resolution of 1/3 octave analysis for data file: III-10.

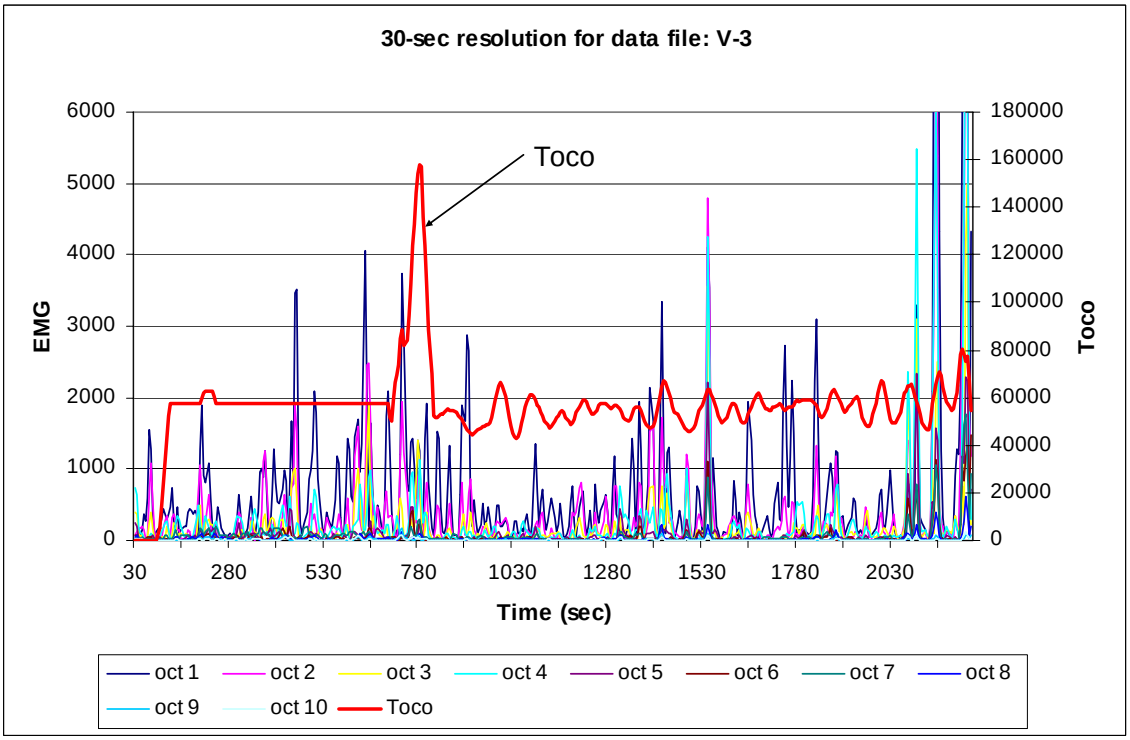

Figure A11. Excel plot of 30-second resolution of 1/3 octave analysis for data file: V-3.

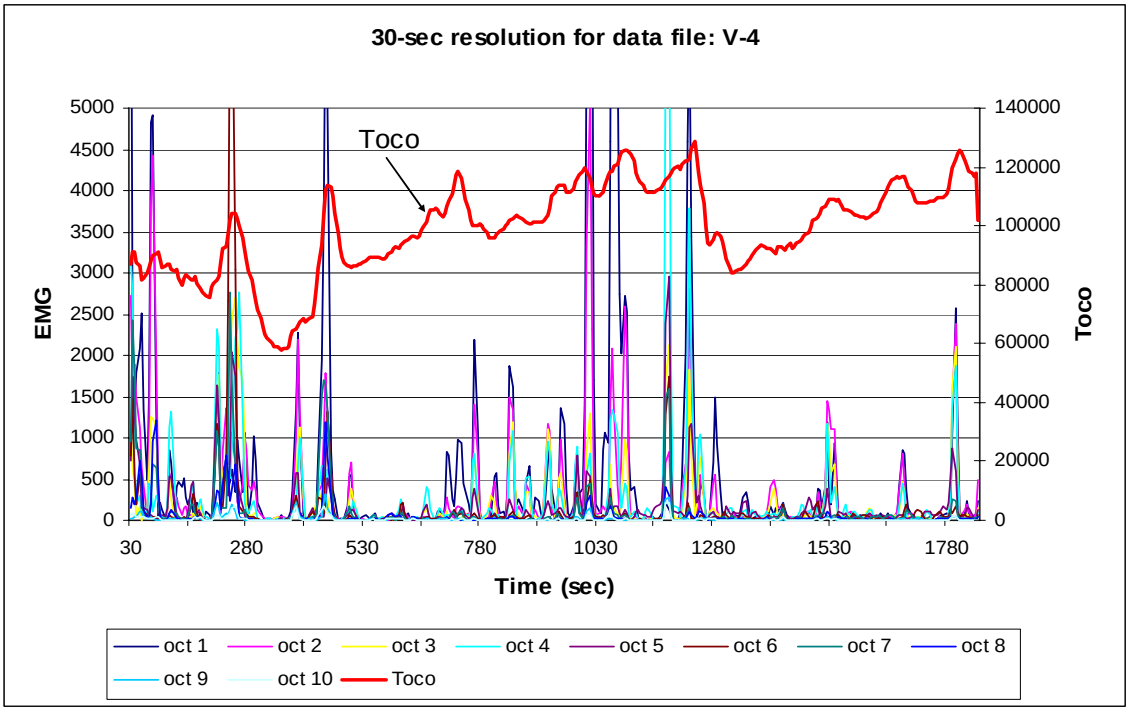

Figure A12. Excel plot of 30-second resolution of 1/3 octave analysis for data file: V-4.

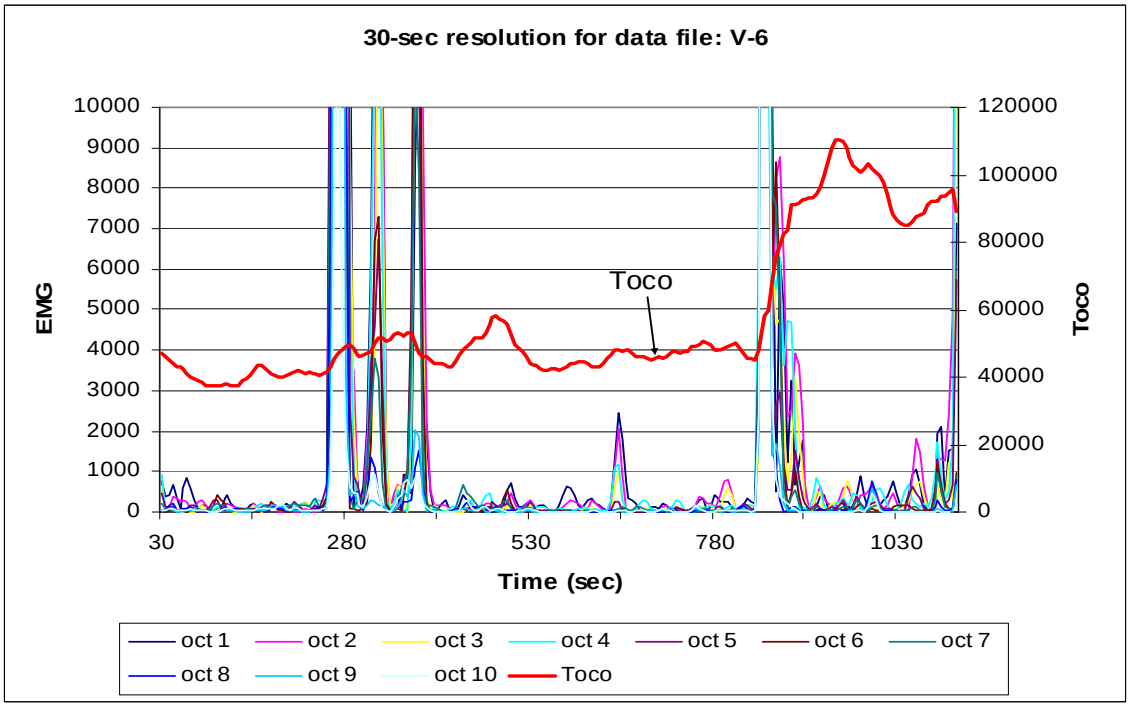

Figure A13. Excel plot of 30-second resolution of 1/3 octave analysis for data file: V-6.

VITA

Name: Lui Cheng

Address: Biomedical Engineering Department
Texas A&M University
233 Zachry Engineering Building
College Station, TX 77843

EDUCATION

M.S. in Biomedical Engineering — December, 2003
Texas A&M University, College Station

B.S. in Electrical Engineering — December, 1998
Texas A&M University, College Station